

INTERNATIONAL JOURNAL OF ENGINEERING INSIGHTS



e-ISSN: 3028-8606

2024

VOLUME 2 | NO.1

<https://doi.org/10.61961/injei.v2i1>



SCI-THOTH



Content

Legal Page	IV
Editorial	VI

Security aspects in the implementation of blockchain in payment gateway transactions in Ecuador	1
Analysis of Degradability of Blackberry (<i>Rubus glaucus</i>) Subjected to Different Storage Conditions	7
PI-Filter compensator for LQG controller aimed to fixed-wings aircrafts	17
Real Time Brain Signals Viewer	25
Early Fault Detection in Paper Machine Motors Using Machine Learning	31

Legal Page

Editor in Chief

Dr. Guillermo Palacios,
University of Zaragoza, Department of Electronic
Engineering and Communications, Spain.

Editorial Board

Ing. Fernando A. Chicaiza, PhD,
Universidad Nacional de San Juan, Argentina.

Ing. Washington Xavier Quevedo Pérez, M.Sc.
INMERSOFT, Ecuador.

Scientific Committee

PhD. Pedro Daniel Bocca,
Universidad Nacional de San Juan, Argentina.

PhD. Pedro Ramos Llorente,
Universidad de Zaragoza, España.

PhD. Viviana Isabel Moya,
Universidad Internacional del Ecuador, Ecuador.

PhD. Ignacio Ayala Chauvin,
Universidad Tecnológica Indoamérica, Ecuador.

PhD. José Luis Varela Aldás,
Universidad Tecnológica Indoamérica, Ecuador.

PhD. David Rivas,
Universidad de las Fuerzas Armadas, Ecuador.

M.Sc. Cristian Mauricio Gallardo Paredes,
Universidad Politécnica de Tomsk, Rusia.

M.Sc. Leonardo, Alves Fagundes-Junior,
Universidade Federal de Viçosa (UFV), Brasil.

M.Sc. Celso. O. Barcelos,
Universidad Federal de Viçosa, Brasil.

M.Sc. Daniel Gomez-Vargas,
Instituto de Automática, UNSJ- CONICET,
Argentina.

M.Sc. Angélica Victoria Guillén Pinargote,
Universidad Técnica de Manabí, Ecuador.

M.Sc. Yadira Maricela Semblantes Claudio,
Universidad de las Fuerzas Armadas, Ecuador.

M.Sc. Edgar Fabián Rivera Guzmán,
Instituto Tecnológico Superior Oriente, Ecuador.

Digital Journal Management Dr. Guillermo Palacios

Style Manager Ing. Fernando A. Chicaiza, PhD

Publication frequency Biannually, November – April

Editorial Sci-thoth
info@injei.sci-thoth.com
(+593) 995763574

Editorial

This volume covers a range of topics within the broad field of engineering, including payment transaction security, physicochemical food analysis, fixed-wing aerial vehicles, brain signal integration with virtual reality, and fault detection in motors using artificial intelligence.

Blockchain technology has transformed transaction methods and is of great collective interest due to its security benefits, such as data protection, immutability, decentralization, authentication, and transparency. These features enhance transaction security and trust. The first paper examines the security aspects of implementing blockchain technology in payment gateway transactions in Ecuador. Blockchain's decentralized nature reduces the risk of cyber-attacks on centralized servers, and its immutability ensures transaction integrity. Moreover, authentication mechanisms like digital signatures and smart contracts ensure that only authorized parties can participate in and validate transactions.

Food security is another critical area in engineering. This journal acknowledges the importance of research aimed at improving and optimizing food production. The second paper evaluates how storage conditions and container types affect blackberries (*Rubus Glaucus*). Two temperatures were analyzed: ambient (19 °C) and refrigeration (4 °C), and three types of containers: low-density polyethylene (LDPE), polypropylene (PP), and polylactic acid (PLA). The results indicated that refrigeration is the best option for maintaining blackberry quality, with PLA excelling in weight preservation and stability, while LDPE was most effective in inhibiting mold growth.

In robotics, fixed-wing aircraft generate lift and propulsion through forward motion, unlike helicopters, which use rotors. Fixed-wing aircraft offer advantages such as greater range, higher speeds, stability in turbulence, and lower operating costs. The

third paper presents a method for improving the smoothness of fixed wing aircraft control using LQG control and PI filter compensation. The paper details experiments conducted through a flight simulator (FlightGear), which allows for testing control algorithms before conducting real-world experiments, providing an efficient and cost-effective development method.

In healthcare, acquiring electroencephalographic signals can be crucial for developing cutting-edge solutions. The fourth article discusses the successful integration of Emotiv EPOC and Unity for real-time visualization of brain signals, significantly advancing the understanding and interaction with brain activity. Real-time visualization offers opportunities in neuroscience, brain-computer interfaces, and cognitive therapy. The paper establishes a robust methodology for acquiring, processing, and graphically representing brain signals in 2D, with results and implications for BCI and cognitive therapy. It also proposes exploring integration with virtual reality and clinical validation to advance real-time brain activity applications.

Finally, integrating artificial intelligence across various fields is essential for developing sophisticated solutions to industrial problems. The fifth paper employs a neural network for early fault detection in the motors of a paper machine within a simulated environment. The study analyzes the torque control loop and collects data to train and validate the model using Direct Torque Control (DTC) simulation of an AC motor in Simscape within Simulink. It considers both normal and faulty operation modes, setting different speed points to gather the necessary data for the model.

These diverse works aim to address gaps in the current state of the art, enriching the literature through the contributions published in this new issue of INJEI.

Dr. Guillermo Palacios

Editor in chief - International Journal of Engineering Insights

Security aspects in the implementation of blockchain in payment gateway transactions in Ecuador

Kerly Naranjo Paez · Renato M. Toasa

Received: 20 Dec 2023 / Accepted: 24 Feb 2024 / Published: 15 May 2024

Abstract: This paper explores the security aspects involved in implementing blockchain technology in payment gateway transactions within the Ecuadorian context. Blockchain technology offers numerous security benefits such as data security, immutability, decentralization, authentication, and transparency. These features contribute to enhancing the overall security and trustworthiness of payment transactions. The decentralized nature of blockchain reduces the risk of cyber attacks targeting centralized servers, while its immutability ensures the integrity of transactions. Additionally, authentication mechanisms such as digital signatures and smart contracts help ensure that only authorized parties can participate in and validate transactions. Furthermore, blockchain's transparency facilitates auditing and compliance with financial regulations. This paper discusses how leveraging blockchain technology can significantly improve security in payment gateway transactions in Ecuador and provides insights into the potential challenges and opportunities associated with its implementation.

Keywords Blockchain · Payment · Security · Transactions · Ecuador

1 Introduction

1.1 Motivation

Currently, payment gateways have certain limitations in terms of security and efficiency compared to solutions based on blockchain. Payment gateways typically centralize transaction data on servers controlled by the entity operating the gateway. This can be a point of

vulnerability, as if these servers are compromised by attackers, there is a risk of financial information and personal data of users being stolen [1].

Traditional payment gateways may be exposed to fraudulent attacks and unauthorized charges. Attackers could exploit vulnerabilities in authentication systems or intercept credit card data to carry out fraudulent transactions [2].

It's important to mention that security in traditional payment gateways has significantly improved over the years, and many companies have implemented robust security measures to protect transactions and user data. However, blockchain technology has the potential to revolutionize the security and efficiency of transactions in payment gateways. Additionally, it offers features such as immutability, transparency, and decentralization that can address some of the challenges mentioned earlier in the context of online transactions [3].


The implementation of blockchain in payment gateways can bring several significant benefits to society [4]. These benefits stem from the unique characteristics of blockchain technology and its ability to enhance security, efficiency, and transparency in online financial transactions. The primary beneficiaries of this proposal are users who make purchases of goods or services online and use their bank cards to complete the order and acquire the goods [5].

In particular, this proposal focuses on Sustainable Development Goal number nine, closely related to innovation, which is considered key to finding a lasting solution that provides security, efficiency, and trust to people when making an online purchase. Additionally, it stimulates innovation in the financial services sector. It can lead to the development of new technological solutions and business models that leverage the security and efficiency features of blockchain.

1.2 Related Works

For the present article, references are taken from various research sources related to the security and pro-

Kerly Naranjo Paez 
Universidad Tecnológica Israel
Quito, Ecuador
E-mail: e1726773169@uisrael.edu.ec

Renato M. Toasa 
Universidad Tecnológica Israel
Quito, Ecuador
E-mail: rtoasa@uisrael.edu.ec

tection of banking information, as well as documents that detail in-depth fundamental concepts of blockchain and its application in different areas. Initially in [6], the authors describe blockchain as a technology that goes far beyond Bitcoin and cryptocurrencies. Although Bitcoin was the first successful application of blockchain, this technology has a wide range of use cases in various industries and fields. Based on the authors' opinion, this statement leads to further exploration of the proposed topic and uncovering the potential of blockchain in payment gateways. Furthermore, in [7], the author examines how blockchain is transforming business models and provides an overview of the practical applications of this technology. There are also proposals for an electricity billing system based on Ethereum blockchain technology and Google's Firebase mobile application development platform. The system aims to enhance efficiency and transparency in the electricity billing process, leveraging the security and decentralization features of Ethereum and the rapid application development capabilities of Firebase [8]. Finally, in [9], the authors describe a blockchain design solution emphasizing the unique features offered by blockchain, such as decentralization, transparency, and security.

The analysis of this solution is closely related to the present work due to the assessment of the needs of implementing blockchain to contribute to the digital transformation of the public sector in Ecuador. The document is organized as follows: Section 1 includes the Introduction, Section 2 the Methodology, Section 3 the Proposal and Section 4 the Conclusions.

2 Methodology

2.1 Focus

A bibliographic, analytical, and direct observational investigation is conducted aiming to identify and comprehend the techniques and strategies employed by payment gateways, while also devising action plans to address the impacts of attacks and prevent future incidents [10].

The aim is to create a proposal that facilitates the adaptation and integration of blockchain technology to enhance transaction security. This proposal aims to ensure that transactions accurately reflect the corresponding information regarding users' actual consumption, while maintaining immutable real-time data records without the need for intermediaries. The methodology also aims to streamline each stage of the process, ensuring efficiency, profitability, and continuous measurement, while preventing fraud. Additionally, it seeks to provide com-

plete and transparent visibility of the process for all parties involved.

2.2 Analysis

According to the research and methodology described above, the proposal to implement blockchain technology in payment gateways in Ecuador, as well as in any other country, is deemed feasible. The analysis conducted through direct observation method entails detailed observation of the processes involved in online payment transactions to identify potential weak points and security risks. The vulnerabilities and threats detected through this method are described below.

Sensitive data leaks: By observing the data input processes in payment gateways, possible vulnerabilities in the protection of sensitive information, such as addresses and personal data, were revealed. The inadvertent exposure of this data could result in identity theft or financial fraud.

Intermediary attacks: Communication between the user, the payment gateway, and the payment service provider can uncover potential points of vulnerability where attackers could intervene and manipulate information during transmission. This could lead to intermediary attacks, such as data interception or identity impersonation.

Authentication vulnerabilities: When observing the user authentication process, effective mechanisms can be evidenced. Nevertheless, with blockchain, the utilization of decentralized digital identities stored in the blockchain can be implemented, ensuring the integrity and immutability of authentication information.

Software security flaws: When examining the user interaction with the payment gateway interface, it is determined that there may be vulnerabilities in the underlying software, such as security breaches, injections of malicious code, or weaknesses in session management.

Social Engineering Attacks: Observing the interactions between the user and the payment gateway reveals potential social engineering tactics used by attackers to deceive users and obtain confidential information, such as login credentials or credit card details.

This analysis enables proactive steps to be taken to mitigate risks and enhance system security. The proposed implementation of blockchain offers various tools and techniques that can be utilized to improve authentication and mitigate vulnerabilities in this critical security process. By implementing measures such as authentication based on blockchain, multifactor authentication, and decentralized identity management, it is possible to create a more robust authentication system

resistant to attacks. Figure 1 depicts the flow of sensitive information in an online payment process.

Fig. 1 Interface of a payment gateway ready for data entry and online payment.

Figure 2 shows the metadata generated when a transaction is carried out, allowing us to highlight the low level of security maintained by these processes.

```
card: {
  number: '4111111111111111',
  bin: '411111',
  type: 'vi',
  transaction_reference: 'DF-522547',
  status: '',
  token: '',
  expiry_year: '2030',
  expiry_month: '11',
  origin: 'Paymentez'
}
[utils/order.js] Transaction marked as paid, shopifyTransactionObj {
  "transaction": {
    "id": "6744106139821",
    "order_id": "4849975328941",
    "kind": "sale",
    "gateway": "Tarjeta de cr\u00e9dito o d\u00e9bito",
    "status": "success",
    "message": null,
    "created_at": "2024-03-11T12:49:25-05:00",
    "test": true,
    "authorization": "DF-522547###1EEtixp",
    "location_id": null,
    "user_id": null,
    "parent_id": "6048341262509",
    "processed_at": "2024-03-11T12:49:25-05:00",
    "device_id": null,
    "error_code": null,
    "source_name": "6943675",
    "receipt": {},
    "amount": "97.40",
    "currency": "USD",
    "payment_id": "#1041.2",
    "total_unsettled_set": {
      "presentment_money": {
        "amount": "0.0",
        "currency": "USD"
      },
      "shop_money": {
        "amount": "0.0",
        "currency": "USD"
      },
      "manual_payment_gateway": true,
      "admin_graphql_api":

```

Fig. 2 Recording a successful transaction through a payment gateway.

3 Proposal

3.1 Current Payment Gateway Phases

Considering the research among payment gateway providers operating in the country, it has been identified that the operational process of a payment gateway involves a series of phases to facilitate a secure online transaction between a buyer and a seller [11]. These phases are detailed below. Figure 3, shows the current operation of a payment gateway.

Transaction initiation: When a customer decides to make an online purchase, they select the products

or services they wish to purchase and proceed to the payment screen.

Choice of payment gateway: The user chooses the payment method they wish to use, such as credit card, debit card, or other methods accepted by the merchant.

Redirection to the payment gateway: Once the payment method is selected, the customer is redirected to the payment gateway screen, where they enter their information to complete the transaction.

Information processing: The payment gateway processes the information provided by the customer and verifies its validity.

Authorization: The payment gateway communicates with the card issuer bank to request authorization and verify if the customer has sufficient funds to make the purchase.

Approval or rejection in the transaction: The card issuer bank or digital wallet provider responds to the payment gateway's authorization request, indicating whether the transaction is approved or rejected.

Transaction confirmation: The payment gateway sends a confirmation message to the merchant's website or application, indicating whether the transaction was successful. If successful, a purchase confirmation is displayed to the customer.

Transaction recording: The payment gateway records the transaction in its system, generating an electronic receipt with details such as the amount, date, merchant, and transaction information.

Settlement and deposit: The payment gateway initiates the settlement process, transferring funds from the customer's account to the merchant. This process may occur immediately or according to a predetermined schedule, depending on the payment gateway and the commercial agreement.

3.2 Blockchain Payment Gateway

The operation of a blockchain payment gateway involves several steps that combine blockchain technology with traditional payment processes [12]. The general components are:

Transaction initiation: The process begins when a customer makes an online purchase and chooses to pay using a payment gateway.

Transaction generation: Once the user selects the payment option, a transaction is generated on the blockchain containing relevant information about the purchase, such as the amount, seller, and buyer.

Digital signature: The buyer digitally signs the transaction using their private key, ensuring the authenticity and integrity of the transaction.

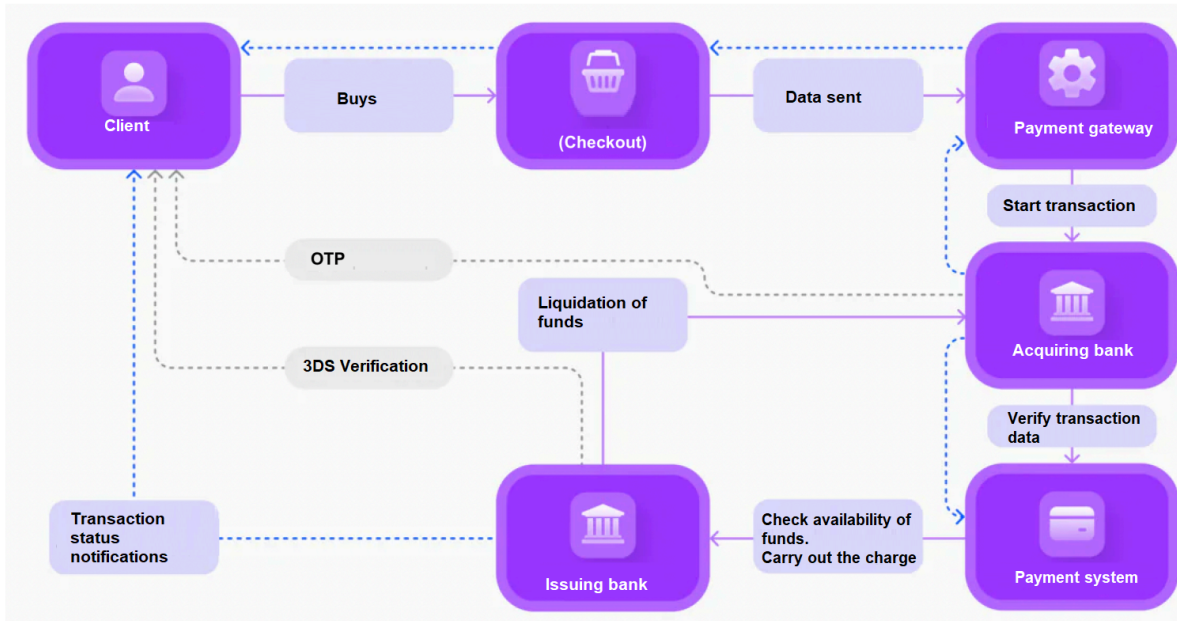


Fig. 3 Operation of an online payment gateway.

Transaction validation: The transaction is transmitted to the blockchain network, where it is validated by network nodes using consensus algorithms. Nodes verify the validity of the transaction and its compliance with the predefined rules of the blockchain.

Inclusion in a block: Once validated, the transaction is included in a block along with other pending transactions. This block is then added to the existing blockchain, creating an immutable record of the transaction.

Payment confirmation: After the block has been added to the blockchain, the transaction is considered confirmed, and the payment process is completed. Confirmation can take several minutes or more, depending on the speed and capacity of the blockchain network used.

Merchant notification: Once the transaction is confirmed, the seller is notified that the payment has been successfully made, and authorization is granted for the delivery of the product or service to the buyer.

Permanent record: The transaction is recorded on the blockchain permanently, providing a transparent and verifiable record of all transactions conducted.

The operation of a payment gateway with blockchain security involves the generation, signing, validation, inclusion, and confirmation of transactions in the blockchain, providing a secure, transparent, and efficient way to process online payments. Figure 4 shows the Payment flow of a blockchain gateway.

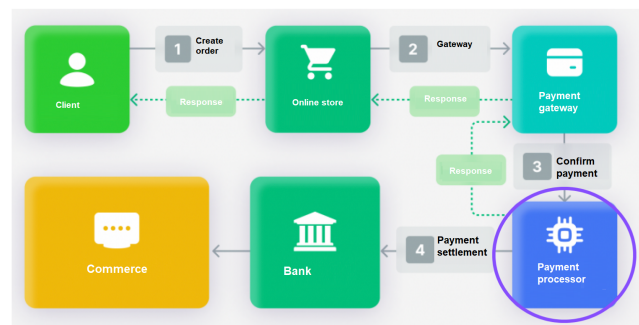


Fig. 4 Payment flow of a blockchain gateway.

3.3 Proposal Structure

A payment gateway plays a crucial role in the online purchasing process, ensuring that financial information is transmitted securely, transactions are authorized, and funds are transferred appropriately between the involved parties. Below is the proposal for the adaptation and implementation of blockchain aimed at securing the transaction process of e-commerce businesses, focusing on data security fundamentals using blockchain technology. Every event or modification of data is written as a new block in a chain, thus creating a certified, settled record, ensuring its integrity and availability [13]. Additionally, if the content is encrypted, reliability is ensured. Figure 5 illustrates the stages comprising the current proposal that will enable the achievement of the objective.

It is proposed to utilize smart contracts and a decentralized network to ensure payment integrity and re-

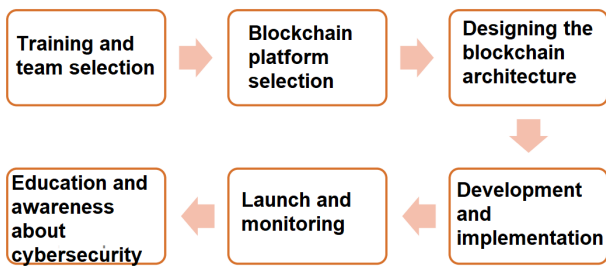


Fig. 5 Proposal designed for blockchain implementation.

duce risks associated with fraud and data manipulation. Additionally, the aim is to eliminate unnecessary intermediaries and streamline settlement processes. This implementation will benefit both merchants and consumers, providing a more secure and reliable payment experience.

3.4 Proposal validation

The proposal was carried out with the support and assessment of two specialists in the field of data security and cybersecurity. The experts believe that a proposal to implement blockchain in payment gateway transactions is a valuable idea. Blockchain technology offers several advantages that could significantly enhance the security, transparency, and efficiency of transactions in payment gateways. However, it is important to note that the successful implementation of blockchain in payment gateways will require careful planning, development, and collaboration among various stakeholders. Additionally, challenges such as scalability, interoperability, and regulation need to be addressed to ensure the long-term success of this proposal. In conclusion, although there are challenges to overcome, the application of blockchain in payment gateway transactions has the potential to generate significant value for the industry and users. The experts validated indicators such as: impact, applicability, conceptualization, relevance, technical quality, feasibility, and relevance, through a scale of 1 - 5, with an average score greater than 4 considered positive, thus validating the proposal and its future implementation in real scenarios.

4 Conclusions

The theoretical foundations on security and blockchain uncovered during the research development enable us to appraise the proposal as it provides a high level of confidence by drawing upon expert sources and books delving into the application of blockchain across various areas beyond the realm of Bitcoin.

The vulnerabilities and threats detected in the flow of a bank transaction through a payment gateway have allowed us to understand that currently, companies providing this service face significant challenges and possibilities of being attacked due to handling sensitive and valuable user information in e-commerce. By designing a proposal that promotes the implementation of blockchain as a security technique in the online payment transaction process, we have paved the way for enhancing security and trust in digital commerce. This proposal not only offers an innovative and effective solution to address security challenges in online transactions but also paves the way for increased adoption and acceptance of blockchain technology in the financial and commercial sectors.

Conflict of interest

The authors declare that they have no conflict of interest.

References

1. M. Di Pierro, "What is the blockchain?" *Computing in Science & Engineering*, vol. 19, no. 5, pp. 92–95, 2017.
2. Sumanjeet, "Emergence of payment systems in the age of electronic commerce: The state of art," in *2009 First Asian Himalayas International Conference on Internet*. IEEE, 2009, pp. 1–18.
3. D. S. W. Khan, "Cyber security issues and challenges in e-commerce," in *Proceedings of 10th international conference on digital strategies for organizational success*, 2019.
4. S.-I. Kim and S.-H. Kim, "E-commerce payment model using blockchain," *Journal of Ambient Intelligence and Humanized Computing*, vol. 13, no. 3, pp. 1673–1685, 2022.
5. Y. Hu, A. Manzoor, P. Ekparinya, M. Liyanage, K. Thilakarathna, G. Jourjon, and A. Seneviratne, "A delay-tolerant payment scheme based on the ethereum blockchain," *IEEE Access*, vol. 7, pp. 33 159–33 172, 2019.
6. D. Tapscott and A. Tapscott, *Blockchain revolution: how the technology behind bitcoin is changing money, business, and the world*. Penguin, 2016.
7. W. Mougayar, *The business blockchain: promise, practice, and application of the next Internet technology*. John Wiley & Sons, 2016.
8. K. M. Hlaing and D. E. Nyaung, "Electricity billing system using ethereum and firebase," in *2019 International Conference on Advanced Information Technologies (ICAIT)*. IEEE, 2019, pp. 217–221.
9. A. R. Ramos Rodríguez, "Análisis de pertinencia de una solución de diseño de bloques de seguridad en transacciones descentralizadas para el gobierno electrónico ecuatoriano." Master's thesis, Quito, Ecuador: Editorial UIS-RAEL, 2023.
10. N. Galí Espelt and J. A. Donaire, "Direct observation as a methodology for effectively defining tourist behavior," *© e-Review of Tourism Research (eRTR), 2010 (Enter 2010 Short papers)*, vol. 1, 5 p., 2010.

11. M. A. Hassan, Z. Shukur, and M. K. Hasan, "An efficient secure electronic payment system for e-commerce," *computers*, vol. 9, no. 3, p. 66, 2020.
12. U. Bodkhe, P. Bhattacharya, S. Tanwar, S. Tyagi, N. Kumar, and M. S. Obaidat, "Blohost: Blockchain enabled smart tourism and hospitality management," in *2019 international conference on computer, information and telecommunication systems (CITS)*. IEEE, 2019, pp. 1–5.
13. I. Yaqoob, K. Salah, R. Jayaraman, and Y. Al-Hammadi, "Blockchain for healthcare data management: opportunities, challenges, and future recommendations," *Neural Computing and Applications*, pp. 1–16, 2022.

License

Copyright (2024) © Kerly Naranjo Paez and Renato M. Toasa.

This text is protected under an international Creative Commons 4.0 license.



You are free to share, copy, and redistribute the material in any medium or format — and adapt the document — remix, transform, and build upon the material — for any purpose, even commercially, provided you comply with the conditions of Attribution. You must give appropriate credit to the original work, provide a link to the license, and indicate if changes were made. You may do so in any reasonable manner, but not in a way that suggests endorsement by the licensor or approval of your use of the work.

[License summary](#) - [Full text of the license](#)


Analysis of Degradability of Blackberry (*Rubus glaucus*) Subjected to Different Storage Conditions


Eduardo Teneda-Ramos · Lorena Cáceres-Miranda · Pedro Escudero-Villa · Esteban Fuentes-Pérez · José Varela-Aldás

Received: 10 Feb 2024 / Accepted: 24 April 2024 / Published: 15 May 2024


Abstract: The purpose of this study was to assess how different storage conditions and types of containers affect blackberries (*Rubus glaucus*), fruits that are particularly susceptible to post-harvest deterioration. Comparisons were made between two temperature conditions: room temperature (19°C) and refrigeration (4°C), and three types of container materials: low-density polyethylene (LDPE), polypropylene (PP), and polylactic acid (PLA). The findings indicated that refrigeration is the most effective strategy for maintaining the quality of blackberries during storage. This method significantly preserved the weight and stability of the fruit, with PLA standing out in this respect. Additionally, a considerable reduction in microbial activity was observed under refrigeration, with LDPE proving to be the most effective at inhibiting mold growth. These results underscore the importance of properly controlling both temperature and container materials type to extend shelf life and preserve the quality of blackberries, which is crucial not only for the food industry, where maintaining freshness and flavor is imperative, but also for consumers who seek high-quality fruit products.

Keywords Storage · Degradability · *Rubus glaucus* · Refrigeration · Maturity index

Eduardo Teneda-Ramos · Lorena Cáceres-Miranda 
SISAU Research Group, Facultad de Ingeniería, Industria y Producción-Universidad Indoamérica
Ambato, Ecuador
eduardo_teneda@outlook.com, lorenacaceres@uti.edu.ec

Pedro Escudero-Villa 
Facultad de Ingeniería, Universidad Nacional de Chimborazo
Riobamba, Ecuador
pedro.escudero@unach.edu.ec

Esteban Fuentes-Pérez 
G+ BioFood and Engineering Group, Department of Food Science and Engineering, Technical University of Ambato
Ambato, Ecuador
e.fuentes@uta.edu.ec

José Varela-Aldás 
Centro de Investigación en Ciencias Humanas y de la Educación—CICHE, Universidad Indoamérica
Riobamba, Ecuador
josevarela@uti.edu.ec

1 Introduction

The growing demand for fresh, high-quality, and long-lasting foods has significantly boosted research and development in this area [1,2]. Fresh fruits and vegetables, vital sources of vitamins, minerals, and antioxidants, suffer physical and microbial deterioration, causing losses of up to 30% during post-harvest and storage stages [3,4]. Specifically, crops such as roots, tubers, and oilseeds experience the highest loss rates at all stages of the supply chain due to their high perishability [5,6]. Fruits, highly susceptible to physiological and physicochemical changes such as weight loss, respiration, transpiration, pulp softening, and alterations in sugar and acidity levels, see their shelf life reduced [7]. In other words, the period during which fresh foods remain suitable for sale and human consumption is limited [8].

Fruits are classified into two categories based on their behavior towards ethylene during ripening: climacteric and non-climacteric [9,10]. Climacteric fruits can continue to ripen after harvest and are capable of producing ethylene, a gas that triggers biochemical and physical changes resulting in complete ripening [11,12]. On the other hand, non-climacteric fruits do not produce ethylene and thus have limited ability to soften or change flavor after harvest, also being more prone to damage during transport and having a shorter shelf life compared to climacteric fruits [13].

Currently, a variety of materials are used to package fresh products, with the use of Polyethylene Terephthalate (PET) and Polystyrene (PS) for rigid containers, and polyolefins for bags, PS for foam trays, and Polyvinyl Chloride (PVC) for wraps standing out [14]. All these materials are derived from petroleum polymers [15] and are essential for ensuring product quality during transport, storage, sale, and use [16]. The packaging industry is currently focused on developing solutions that extend the shelf life of foods, ensuring their nutritional, microbiological, and organoleptic quality [17, 18,19].

The Blackberry (*Rubus glaucus*) is a non-climacteric fruit valued for its nutritional and antioxidant properties, pleasant color and flavor, and the health benefits it provides to humans [20, 21, 22, 23]. However, its quality rapidly deteriorates after harvest, and it has a shelf life of only 3 to 5 days, with losses that can reach up to 70% due to its high water content and active metabolism, as well as its susceptibility to mechanical damage and microbial attack, requiring special care during storage [24, 25, 26, 27, 28].

Various post-harvest initiatives have been proposed to improve the conservation of blueberries, raspberries, and blackberries throughout the entire supply chain [29]. These include physicochemical methods such as heat treatments, ultraviolet radiation application, sanitization, and edible coatings, as well as packaging solutions such as Modified Atmosphere Packaging (MAP) and active packaging with ethylene control [30]. The combined application of these technologies has contributed to extending the shelf life of berries, meeting the growing global demand, and improving consumer satisfaction [31, 32].

The use of various packaging materials, both bio-based and petroleum-derived, oriented polylactic acid (OPLA) and biaxially-oriented polystyrene (OPS), has been suggested [33] to reduce the mechanical impact on “Cancaska” and “Chester” blackberry varieties. Although these fruits lost weight, altered their solid content and pH, their nutritional characteristics, according to US standard No. 1, remained suitable for commercialization for more than 12 days at 3 °C [14].

In contrast to using single-material packaging, initiatives have also been explored to assess the impact on the quality and shelf life of blackberries stored at 4 °C for 20 days in packaging with a prebiotic edible coating based on starch with nystatin addition [34, 35, 36]. This coating has reduced microbial contamination compared to the control blackberries and those coated with starch only. The starch and starch-nystatin coatings have proven effective in delaying pH increase, maintaining firmness, and the anthocyanin content of the fruits, which has improved their market acceptance [37].

With the goal of assessing the degradability of Blackberry in polymeric packaging, this study experimentally investigated the fruit’s characteristics under different environmental and packaging conditions. The effect of storing the fruit in Low-Density Polyethylene (LDPE), Polypropylene (PP), and Polylactic Acid (PLA) packaging under laboratory and refrigeration conditions was analyzed. Analyses of the fruit’s physicochemical and microbiological properties were conducted. The document is organized as follows: Section 1 includes the Introduction, Section 2 the Methodology, Section 3 the

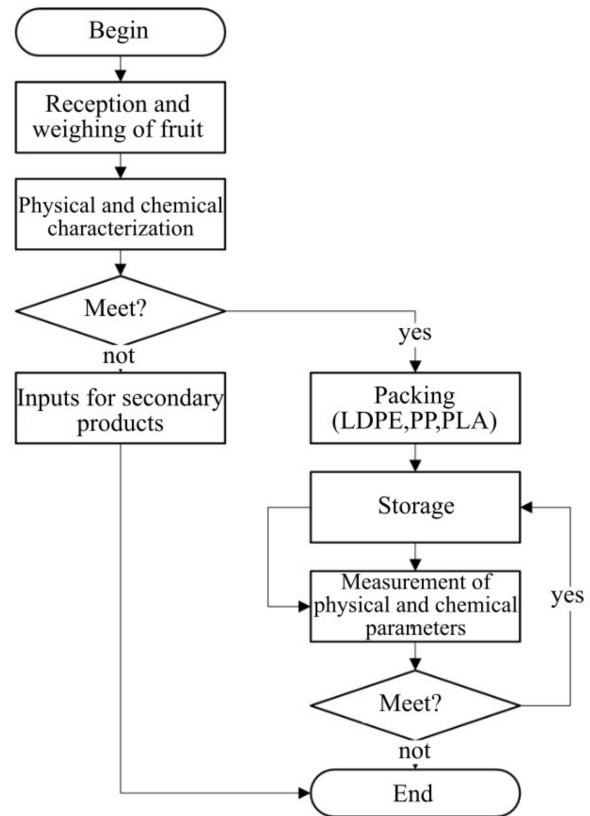


Fig. 1 General outline of the experiment.

Results, Section 4 the Discussion, and Section 5 the Conclusions.

2 Material and Methods

The methodology used in this research starts with the harvesting process, followed by weighing, characterization, packaging, and concludes with a physicochemical analysis after the experiment. Figure 1 shows a general schematic of the procedure.

2.1 Description of the experiment environment

The Basic Sciences Laboratory at Universidad Indoamérica served as the venue for conducting the experiment on the ripeness index of the Blackberry. This study focused on assessing the fruit’s response under two different storage conditions: in a laboratory setting at 19.0 degrees Celsius with a relative humidity of 59%, and in a refrigeration chamber at 4 degrees Celsius with a relative humidity of 97%. These conditions aim to mimic real storage scenarios, allowing for the analysis of the fruit’s behavior in both contexts [38, 39]. The lighting in the laboratory was maintained constant at 500 lux,

ensuring an appropriate environment for all necessary measurements, which contributed to the reliability and validity of the results obtained.

2.2 Reception and weighing

For the harvest, Blackberries at ripeness levels 3 and 4 were selected, all of uniform size and free from physical damage or microbial contamination [40]. These blackberries were picked during the early hours of the experiment day to ensure their freshness and prevent chemical or microbiological changes that could influence the results. The harvesting was conducted by berry producer associations in Canton Tisaleo, Ecuador. Containers with a capacity of 7 kg were used to transport the product from the cultivation area to the laboratory, taking an average time of 30 minutes.

2.3 Physicochemical characterization

As initial physicochemical parameters of the blackberries, titratable acidity was determined using the potentiometric method in accordance with the methodology established by ISO 750:1998, Fruit and vegetable products - Determination of titratable acidity - ISO 750:1998, and the results were expressed as a percentage of citric acid (%). Soluble solids were measured following the instructions of ISO 2173:2003, Determination of soluble solids - Refractometric method ISO 2173:2003, using a refractometer. The maturity index was calculated by the ratio of soluble solids to acidity [43].

2.4 Packaging

To begin the study, the blackberries were packaged in three different types of containers: LDPE, PP, and PLA as seen in Figure 2. In addition, the characteristics of the containers are detailed in Table 1.

3 Results

3.1 Morphological analysis

The Blackberry can reach lengths of up to 3.5 cm and diameters of up to 2.3 cm, with a weight ranging between 6.1 and 7.8 g. These fruits are generally conical in shape. The seed, wedge-shaped with a reticulated surface, measures between 4 and 6 mm in length and about 2 mm in width. Each fruit contains around 70-85 drupes, with yields that can reach up to 15 t/ha

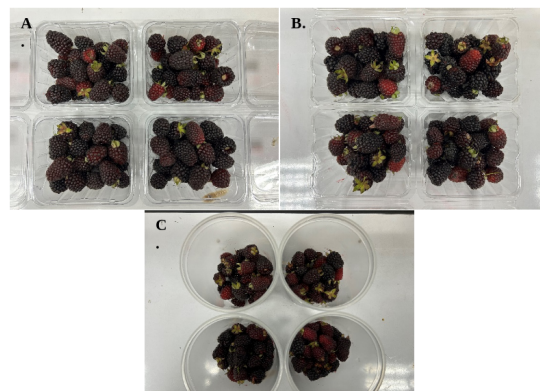


Fig. 2 Experiment containers: A). LDPE, B). PP, C). PLA

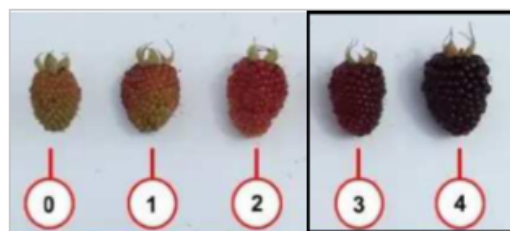


Fig. 3 Colorimetry according to the state of maturity of the Blackberry.

[44, 45]. In Ecuador, the cultivation of blackberries, primarily represented by *Rubus glaucus* and other species of the *Rubus Genus*, is spread throughout the Inter-Andean valley, specifically at altitudes ranging from 2000 to 3100 meters above sea level. This crop plays a significant role in the local economy due to its high demand both for fresh consumption and processing [46, 47]. Blackberries are cultivated in the provinces of Tungurahua, Cotopaxi, Bolívar, Chimborazo, Pichincha, Imbabura, and Carchi, with average annual yields increasing from 2.19 t/ha in 2000 to 6.80 t/ha in 2016, primarily destined for fresh consumption and the agro-industry. Although producers are interested in varieties that offer high fruiting, yield, and quality, blackberry cultivation has not yet reached the desired development in the country, partly due to the lack of promising materials that improve or complement traditionally cultivated ones [48, 49, 50].

According to Ecuatoriana Nte Inen 2204, the color of the Blackberry, based on its ripeness, follows a color scale ranging from 0 to 4, as detailed in Table 2.

In this research, blackberries in color scale 3 and 4 were used; Figure 3 Ecuatoriana Nte Inen 2204, shows the colorimetry of the blackberries.

Table 1 Storage materials specifications

Material	Description	Dimensions (mm)	Weight (g)	Closed type
LDPE	This material is notable for its flexibility, impact resistance, and translucence, attributes that stem from its branched-chain structure. This structure gives it a low density, making it lightweight and easily moldable. Its widespread use in the production of bags, containers, and toys is due to its versatility and excellent chemical resistance [41].	10.95x95,00x61.00	18.28	Lid with pressure and hinge
PP	It is a type of thermoset plastic known for its strength, lightness, and versatility. Commonly used in packaging, textiles, and automotive components, its durability and malleability make it extremely popular across various industries [42].	10.95x95.00x61.00	19.10	Lid with pressure and hinge
PLA	PLA is a bioplastic derived from renewable sources such as cornstarch or sugarcane. It is noted for its biodegradability and compostability, making it an environmentally friendly option. Its versatile properties make it suitable for the manufacture of packaging, 3D printing filaments, and disposable products.	Diameter 1: 99.00 x Diameter 2: 112.00 x 120.00	19.38	Lid with pressure and hinge

Table 2 Color scale according to state of maturity.

Color	Description
0	Full green fruit or with few brown drupes because of exposure to light with well-formed drupes.
1	Light green fruit with some pink or red drupes.
2	Red fruit with some yellow drupes.
3	Intense red fruit with some purple drupes.
4	Dark purple, almost black fruit.

3.2 Physicochemical evaluation

Figure 4 displays the results of the weight of the blackberries according to the type of packaging and storage temperature. It is observed that blackberries stored at refrigeration temperature (4°C) maintain a slightly higher weight compared to those stored at laboratory temperature (19°C). This suggests that lower temperatures help to slow down weight loss in blackberries, a phenomenon associated with a decrease in respiration rate and fruit degradation.

Figure 5 shows the results of the weight variable according to the type of study environment. Under laboratory temperature conditions (19°C), blackberries stored in LDPE and PLA tend to maintain a higher weight compared to those stored in PP. However, under refrigeration conditions (4°C), the weight differences between the different types of packaging are less significant. This

suggests that low temperatures may minimize the differences in air permeability and moisture between different types of packaging.

Figure 6 presents the results of the Maturity Index according to the type of packaging and storage temperature. A decrease in the maturity index over time is observed under both temperature conditions. However, blackberries stored at refrigeration temperature (4°C) tend to maintain a slightly higher maturity index compared to those stored at laboratory temperature (19°C). This suggests that refrigeration helps to slow down the degradation process of the blackberries.

Figure 7 presents the results of the Maturity Index according to the type of study environment. It was observed that PLA outperformed other materials such as LDPE and PP in terms of fruit stability, particularly under refrigeration conditions. This suggests that PLA has effective barrier properties against moisture and gas loss, which is beneficial for fruit preservation. At room temperature, LDPE maintained a higher maturity index, indicating a greater ability to delay fruit degradability.

3.3 Microbiological evaluation

Figure 8 displays the microbiological results according to the type of study environment. Optimal storage conditions for blackberries were evaluated in relation to microbial activity. The results highlighted how temper-

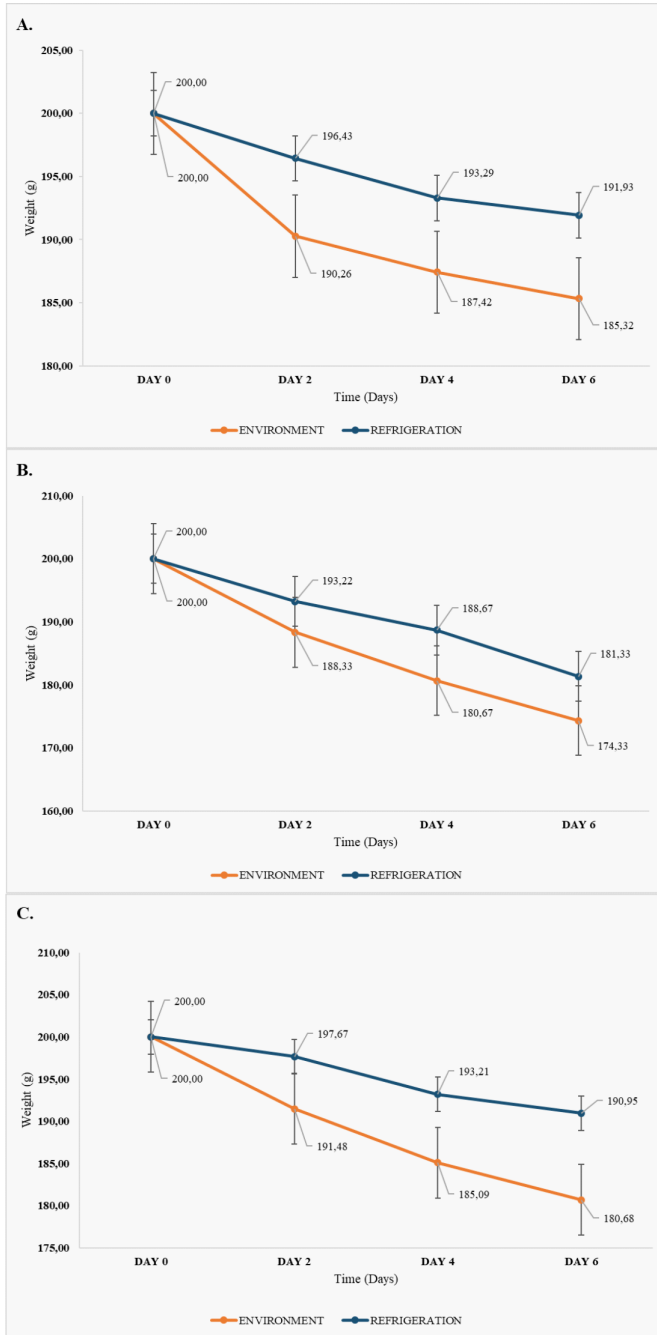


Fig. 4 Weight variation results: A.) LDPE, B.) PP, C.) PLA.

ature and the type of packaging influence this activity. At room temperature, the conditions favor the development of microbial activity, primarily due to the barrier properties of the polymer used. In contrast, under refrigeration conditions (4°C), all packaging materials demonstrated a significant reduction in microbial activity.

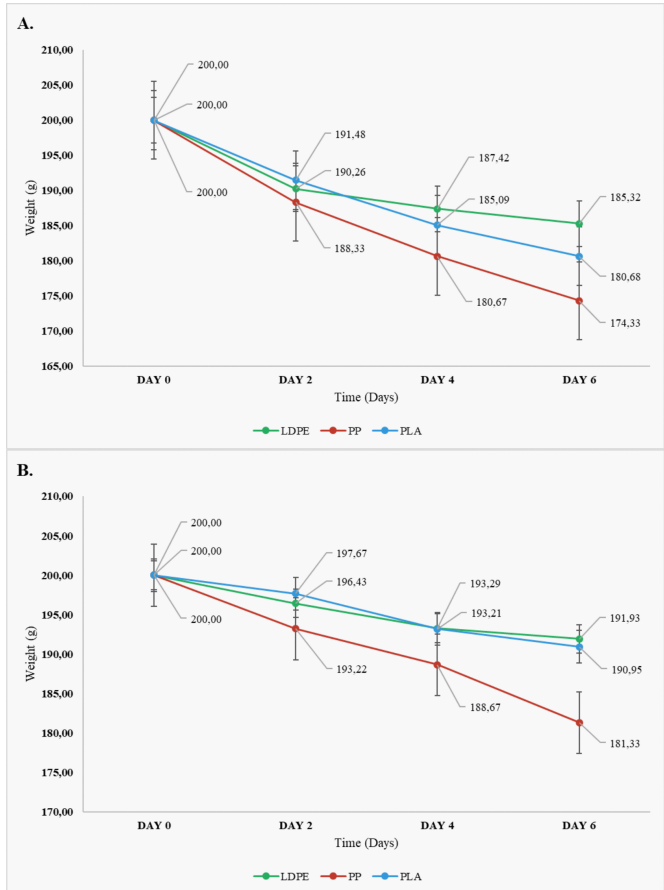


Fig. 5 Results of weight variation according to the type of environment: A.) Environment, B.) Refrigeration.

4 Discussion

When comparing temperatures, it was found that refrigeration (4°C) is more effective for preserving the quality of blackberries compared to laboratory temperature (19°C). This is due to the reduction in the respiration and transpiration rates of the fruit, which is crucial for non-climacteric fruits that do not experience a peak in enzymatic activity during ripening [51]. Nonetheless, these enzymatic activities persist and can influence changes in the texture and flavor of the fruit [52,53]; lower temperatures slow these reactions.

Under refrigeration conditions, PLA outperformed other types of packaging (LDPE and PP) in terms of weight retention and maturity index stability. This indicates that PLA possesses superior barrier properties against moisture and gas loss, benefiting fruit preservation [54]. At room temperature, although LDPE and PP had similar performance in weight retention [55], LDPE maintained a higher maturity index, suggesting a better ability to delay ripening [56].

The high relative humidity in refrigeration (97%) helped reduce weight loss due to the smaller difference

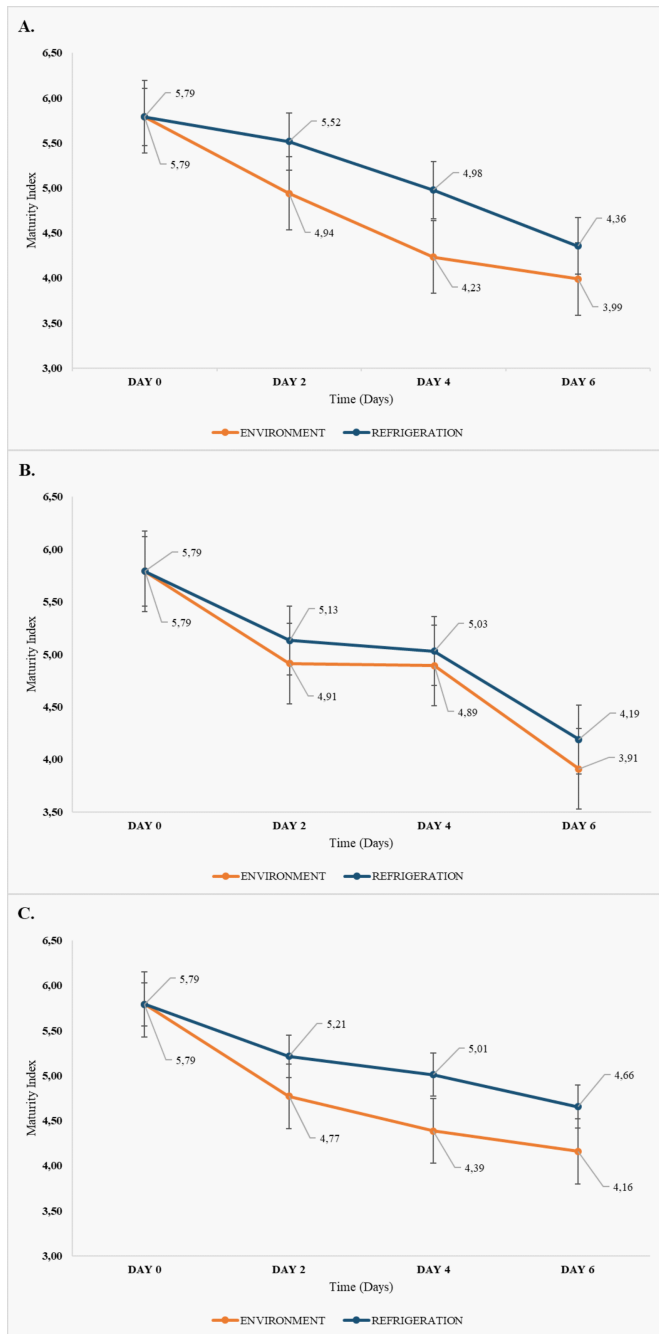


Fig. 6 Results of the variation in the Maturity Index according to the type of packaging and storage environment: A.) LDPE, B.) PP, C.) PLA.

between the moisture content of the fruit and the environment, thus reducing transpiration. In summary, the ideal storage for blackberries depends both on temperature and packaging material. PLA stands out as the most promising material under controlled refrigeration conditions, while LDPE provides better results at room temperature [57]. These findings underscore the importance of considering the interactions between en-

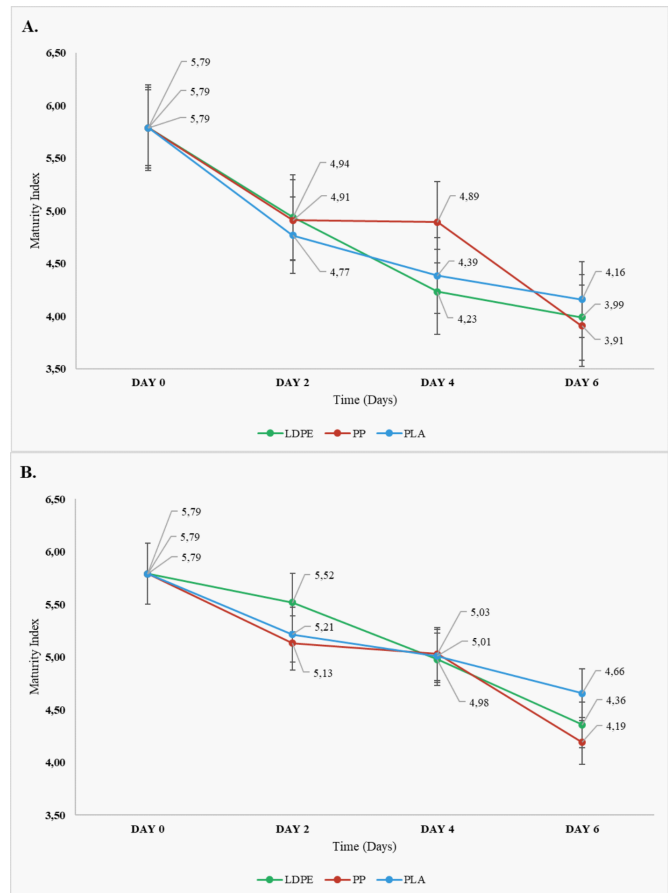


Fig. 7 Results of variation of the Maturity Index according to the environment: A.) Environment, B.) Refrigeration.

vironmental factors and packaging type to maximize the shelf life and postharvest quality of blackberries.

Optimal storage conditions for blackberries were also analyzed in terms of microbial activity. At room temperature (59% relative humidity), the environment is more conducive to microbial development. PLA proved to be more effective in inhibiting mold growth, followed by LDPE and PP, due to its barrier properties that limit moisture and gas transfer, creating a less favorable environment for microbial growth [58,10].

In refrigeration (4°C), all materials showed a significant reduction in microbial activity. The permeability to oxygen and water vapor of the different packaging types can influence the amount of mold present [59,60]. LDPE, being less permeable, provides a more effective barrier against the entry of mold spores from the outside. Although PLA initially shows less mold, it can become less effective over time due to its greater permeability, allowing more spore entry [61,62]. The high relative humidity in refrigeration helps maintain turgor and reduce fruit dehydration, decreasing osmotic stress and, therefore, susceptibility to microbial attack. The combination of low temperature and high relative hu-

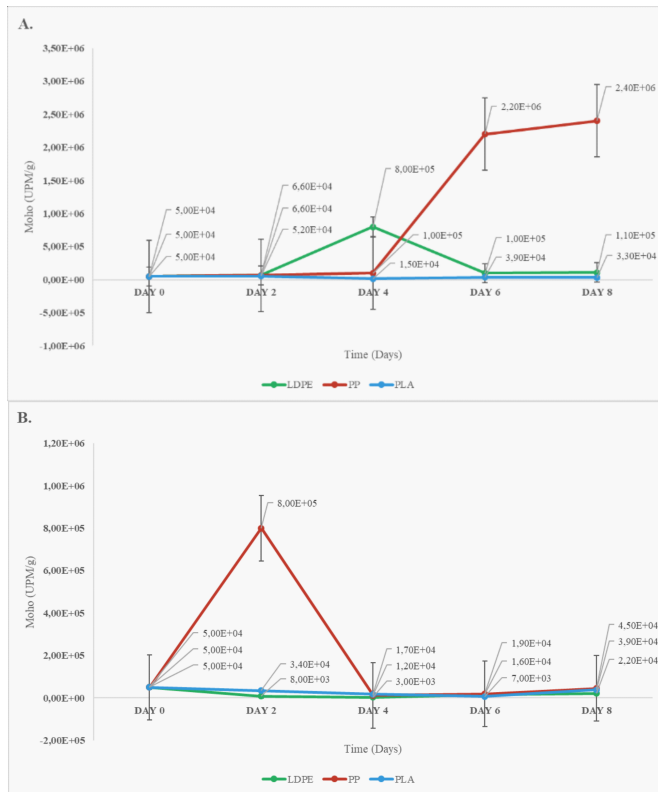


Fig. 8 Results of the microbiological evaluation by environment: A.) Environment, B.) Refrigeration.

midity in refrigeration seems to be the most beneficial for preserving postharvest quality and minimizing microbial activity in blackberries. These findings highlight the importance of integrated control of packaging type and environmental conditions to extend shelf life and maintain the quality of non-climacteric fruits.

5 Conclusions

The characteristics of blackberries (*Rubus glaucus*) were evaluated under various environmental and packaging conditions to analyze their impact on the physicochemical and microbiological properties of the fruit. The results provided valuable information for the development of effective storage and preservation strategies. In terms of physicochemical characteristics, it was found that refrigeration better preserves the quality of blackberries compared to room temperature. The reduction in the fruit's respiration and transpiration rates at lower temperatures significantly contributed to weight retention and stability of the maturity index, suggesting that refrigeration, combined with appropriate packaging, extends shelf life and maintains the quality of blackberries during storage.

Regarding microbiological characteristics, it was demonstrated that both temperature and type of packaging significantly affect microbial activity in blackberries. At room temperature, conditions favor microbial development; PLA was the most effective material in reducing mold growth, followed by LDPE and PP. Under refrigeration, a significant reduction in microbial activity was observed in all packaging types, with LDPE standing out for its ability to provide an effective barrier against the entry of mold spores from the outside.

A limitation of this study is the lack of analysis of parameters such as antioxidant content, texture, or flavor of the fruit. Including these parameters could provide a more comprehensive understanding of how different storage and packaging conditions affect fruit quality.

Conflict of interest

The authors declare that they have no conflict of interest.

References

1. W. Wang, Z.-J. Ni, K. Thakur, S.-Q. Cao, and Z.-J. Wei, "Recent update on the mechanism of hydrogen sulfide improving the preservation of postharvest fruits and vegetables," *Current Opinion in Food Science*, vol. 47, p. 100906, 2022. [Online]. Available: <https://www.sciencedirect.com/science/article/pii/S2214799322001084>
2. J. A. Toscano Ávila, D. A. Terán, A. Debut, K. Vizuete, J. Martínez, and L. A. Cerda-Mejía, "Shelf life estimation of blackberry (*rubus glaucus* benth) with bacterial cellulose film coating from *komagataeibacter xylinus*," *Food Science & Nutrition*, vol. 8, no. 4, pp. 2173–2179, 2020. [Online]. Available: <https://onlinelibrary.wiley.com/doi/abs/10.1002/fsn3.1525>
3. M. Palumbo, G. Attolico, V. Capozzi, R. Cozzolino, A. Corvino, M. L. V. de Chiara, B. Pace, S. Pelosi, I. Ricci, R. Romaniello, and M. Cefola, "Emerging postharvest technologies to enhance the shelf-life of fruit and vegetables: An overview," *Foods*, vol. 11, no. 23, 2022. [Online]. Available: <https://www.mdpi.com/2304-8158/11/23/3925>
4. G. N. Tenea, P. Reyes, D. Molina, and C. Ortega, "Pathogenic microorganisms linked to fresh fruits and juices purchased at low-cost markets in ecuador, potential carriers of antibiotic resistance," *Antibiotics*, vol. 12, no. 2, 2023. [Online]. Available: <https://www.mdpi.com/2079-6382/12/2/236>
5. U. D. Corato, "Improving the shelf-life and quality of fresh and minimally-processed fruits and vegetables for a modern food industry: A comprehensive critical review from the traditional technologies into the most promising advancements," *Critical Reviews in Food Science and Nutrition*, vol. 60, no. 6, pp. 940–975, 2020, pMID: 30614263. [Online]. Available: <https://doi.org/10.1080/10408398.2018.1553025>
6. O. Chauhan, S. Lakshmi, A. Pandey, N. Ravi, N. Gopalan, and R. Sharma, "Non-destructive quality

- monitoring of fresh fruits and vegetables,” *Defence Life Science Journal*, vol. 2, p. 103, 05 2017.
7. S. Sinha, M. Kader, M. A. Jiku, A. Rahaman, A. Singha, M. Faruquee, and M. Alam, “Post-harvest assessment of fruit quality and shelf life of two elite tomato varieties cultivated in bangladesh,” *Bulletin of the National Research Centre*, vol. 43, p. 185, 12 2019.
 8. Onethird, “The ultimate guide to fresh produce shelf life prediction,” pp. 1–17, 2022. [Online]. Available: <https://onethird.io/ultimate-guide-to-fresh-produce-shelf-life-prediction>
 9. M. E. Martínez-González, R. Balois-Morales, I. Alia-Tejacal, M. A. Cortes-Cruz, Y. A. Palomino-Hermosillo, G. G. López-Gúzman, M. E. Martínez-González, R. Balois-Morales, I. Alia-Tejacal, M. A. Cortes-Cruz, Y. A. Palomino-Hermosillo, and G. G. López-Gúzman, “Poscosecha de frutos: maduración y cambios bioquímicos,” *Revista mexicana de ciencias agrícolas*, vol. 8, no. SPE19, pp. 4075–4087, dec 2017. [Online]. Available: http://www.scielo.org.mx/scielo.php?script=sci_arttext&pid=S2007-09342017001104075&lng=es&nrm=iso&tlng=eshttp://www.scielo.org.mx/scielo.php?script=sci_abstract&pid=S2007-09342017001104075&lng=es&nrm=iso&tlng=es
 10. M. Cabrera, V. Peralta, F. Rodríguez, T. Herrera, and J. Herrera, “Evaluación “in vitro” de la actividad antifúngica del aceite esencial de canela (*cinnamomum zeylanicum*) sobre *botrytis* sp aislado de mora de castilla (*rubus glaucus*),” *European Scientific Journal ESJ*, vol. 15, 04 2019.
 11. A. Martiñón, S. Chavez, C. Veloz, J. Espinosa, and D. Guerra-Ramírez, “Extractos de persea americana mill. que retrasan maduración en frutos de aguacate,” *Revista Mexicana de Ciencias Agrícolas*, vol. 9, pp. 1639–1650, 12 2018.
 12. M. J. A., M. ., and J. ., “Evaluación fisicoquímica y antioxidante de naranjilla (*solanum quitoense* lam.) durante la maduración,” *Revista Iberoamericana de Tecnología Postcosecha*, vol. 22, 2021. [Online]. Available: <https://www.redalyc.org/articulo.oa?id=81369610003>
 13. C. Figueroa, C. Concha, N. Figueroa, and G. Tapia, “Fru-tilla chilena nativa - *fragaria chiloensis*,” 01 2018.
 14. M. Joo, N. Lewandowski, R. Auras, J. Harte, and E. Almenar, “Comparative shelf life study of black-berry fruit in bio-based and petroleum-based con-tainers under retail storage conditions,” *Food Chem-istry*, vol. 126, no. 4, pp. 1734–1740, 2011. [On-line]. Available: <https://www.sciencedirect.com/science/article/pii/S0308814610016924>
 15. C. G. Otoni, R. J. Avena-Bustillos, H. M. C. Azeredo, M. V. Lorevice, M. R. Moura, L. H. C. Mattoso, and T. H. McHugh, “Recent advances on edible films based on fruits and vegetables—a review,” *Comprehensive Reviews in Food Science and Food Safety*, vol. 16, no. 5, pp. 1151–1169, 2017. [Online]. Available: <https://ift.onlinelibrary.wiley.com/doi/abs/10.1111/1541-4337.12281>
 16. T. Ahmed, M. Shahid, F. Azeem, I. Rasul, A. A. Shah, M. Noman, A. Hameed, N. Man-zoor, I. Manzoor, and S. Muhammad, “Biodegra-dation of plastics: current scenario and future prospects for environmental safety,” *Environmental Science and Pollution Research*, vol. 25, no. 8, pp. 7287–7298, mar 2018. [Online]. Available: <https://link.springer.com/article/10.1007/s11356-018-1234-9>
 17. M. K. Verma, S. Shakya, P. Kumar, J. Madhavi, J. Murugaiyan, and M. V. Rao, “Trends in packaging material for food products: historical background, current scenario, and future prospects,” *Journal of Food Science and Technology*, vol. 58, no. 11, pp. 4069–4082, nov 2021. [Online]. Available: <https://link.springer.com/article/10.1007/s13197-021-04964-2>
 18. N. K. Dubey and R. Dubey, “Chapter 27 - edible films and coatings: An update on recent advances,” in *Biopolymer-Based Formulations*, K. Pal, I. Banerjee, P. Sarkar, D. Kim, W.-P. Deng, N. K. Dubey, and K. Majumder, Eds. Elsevier, 2020, pp. 675–695. [Online]. Available: <https://www.sciencedirect.com/science/article/pii/B9780128168974000278>
 19. A. Prakash, R. Baskaran, N. Paramasivam, and V. Vadivel, “Essential oil based nanoemulsions to improve the microbial quality of minimally processed fruits and vegetables: A review,” *Food Research International*, vol. 111, pp. 509–523, 2018. [On-line]. Available: <https://www.sciencedirect.com/science/article/pii/S0963996918304356>
 20. Z. Diaconeasa, C. I. Iuhas, H. Ayvaz, D. Ruginã, A. Stanilã, F. Dulf, A. Bunea, S. A. Socaci, C. Socaciu, and A. Pinteã, “Phytochemical characterization of com-mercial processed blueberry, blackberry, blackcurrant, cranberry, and raspberry and their antioxidant activity,” *Antioxidants*, vol. 8, no. 11, 2019. [Online]. Available: <https://www.mdpi.com/2076-3921/8/11/540>
 21. F. Velázquez-Contreras, N. García-Caldera, J. D. Padilla de la Rosa, D. Martínez-Romero, E. Núñez-Delgado, and J. A. Gabaldón, “Effect of pla active packag-ing containing monoterpeno-cyclodextrin complexes on berries preservation,” *Polymers*, vol. 13, no. 9, 2021. [Online]. Available: <https://www.mdpi.com/2073-4360/13/9/1399>
 22. C. M., M. J. ., A. ., A. ., and A. ., “Efecto del uso combinado de radiaciÓn uv - c y atmÓsfera modificada sobre el tiempo de vida Útil de mora de castilla (*rubus glaucus*) sin espinas,” *Revista Iberoamericana de Tecnología Postcosecha*, vol. 17, pp. 71–78, 2016. [Online]. Available: <https://www.redalyc.org/articulo.oa?id=81346341010>
 23. S. Santos, L. Rodrigues, S. Costa, and G. Madrona, “Antioxidant compounds from blackberry (*rubus fruticosus*) pomace: Microencapsulation by spray-dryer and ph stability evaluation,” *Food Packaging and Shelf Life*, vol. 20, p. 100177, 2019. [On-line]. Available: <https://www.sciencedirect.com/science/article/pii/S2214289417301989>
 24. M. Hadadinejad, K. Ghasemi, and A. A. Mohammadi, “Effect of storage temperature and packaging material on shelf life of thornless blackberry,” *International Journal of Horticultural Science and Technology*, vol. 5, no. 2, pp. 265–275, 2018.
 25. E. L. Potma da Silva, T. C. de Carvalho, R. Antonio Ayub, and M. C. Menezes de Almeida, “Blackberry extend shelf life by nanocellulose and vegetable oil coat-ing,” *Horticulture International Journal*, vol. Volume 4, no. Issue 2, pp. 54–60, apr 2020. [Online]. Avail-able: <https://medcraveonline.com/HIJ/HIJ-04-00158.phphttps://medcraveonline.com/HIJ/HIJ-04-00158.pdf>
 26. C. Villegas and W. Albarracín, “Edible coating applica-tion and effect on blackberry (*rubus glaucus* benth) shelf life,” *Vitae*, vol. 23, pp. 202–209, 09 2016.
 27. Sandhya, “Modified atmosphere packaging of fresh produce: Current status and future needs,” *LWT - Food Science and Technology*, vol. 43, no. 3, pp. 381–392, 2010. [Online]. Available: <https://www.sciencedirect.com/science/article/pii/S0023643809001546>

28. A. Ascencio-Arteaga, S. Luna-Suárez, J. G. Cárdenas-Valdovinos, E. Oregel-Zamudio, G. Oyoque-Salcedo, J. A. Ceja-Díaz, M. V. Angoa-Pérez, and H. G. Mena-Violante, "Shelf life of blackberry fruits (*rubus fruticosus*) with edible coatings based on candelilla wax and guar gum," *Horticulturae*, vol. 8, no. 7, 2022. [Online]. Available: <https://www.mdpi.com/2311-7524/8/7/574>
29. N. K. Huynh, M. D. Wilson, A. Eyles, and R. A. Stanley, "Recent advances in postharvest technologies to extend the shelf life of blueberries (*Vaccinium* sp.), raspberries (*Rubus idaeus* L.) and blackberries (*Rubus* sp.)," *Journal of Berry Research*, vol. 9, no. 4, pp. 687–707, jan 2019.
30. M. D. Wilson, R. A. Stanley, A. Eyles, and T. Ross, "Innovative processes and technologies for modified atmosphere packaging of fresh and fresh-cut fruits and vegetables," *Critical reviews in food science and nutrition*, vol. 59, no. 3, pp. 411–422, feb 2019. [Online]. Available: <https://pubmed.ncbi.nlm.nih.gov/28891686/>
31. P. Joshi, N. Becerra-Mora, A. Y. Vargas-Lizarazo, P. Kohli, D. J. Fisher, and R. Choudhary, "Use of edible alginate and limonene-liposome coatings for shelf-life improvement of blackberries," *Future Foods*, vol. 4, p. 100091, 2021. [Online]. Available: <https://www.sciencedirect.com/science/article/pii/S2666833521000812>
32. Y. Tumbarski, N. Petkova, M. Todorova, I. Ivanov, I. De-seva, D. Mihaylova, and S. Ibrahim, "Effects of pectin-based edible coatings containing a bacteriocin of bacillus methylotrophicus bm47 on the quality and storage life of fresh blackberries," *Italian Journal of Food Science*, vol. 32, pp. 420–437, 05 2020.
33. N. R. Giuggioli, R. Briano, and C. Peano, "Packaging in the fresh fruit and vegetable supply chain: Innovation and sustainability," *Italus Hortus*, vol. 25, no. 1, pp. 23–38, 2018.
34. G. T. Bersaneti, S. H. Prudencio, S. Mali, and M. A. Pedrine Colabone Celligoi, "Assessment of a new edible film biodegradable based on starch-nystose to increase quality and the shelf life of blackberries," *Food Bioscience*, vol. 42, p. 101173, 2021. [Online]. Available: <https://www.sciencedirect.com/science/article/pii/S2212429221002984>
35. M. V. Alvarez, A. G. Ponce, and M. R. Moreira, "Influence of polysaccharide-based edible coatings as carriers of prebiotic fibers on quality attributes of ready-to-eat fresh blueberries," *Journal of the Science of Food and Agriculture*, vol. 98, no. 7, pp. 2587–2597, 2018. [Online]. Available: <https://onlinelibrary.wiley.com/doi/abs/10.1002/jsfa.8751>
36. R. Porat, A. Lichter, L. A. Terry, R. Harker, and J. Buzby, "Postharvest losses of fruit and vegetables during retail and in consumers' homes: Quantifications, causes, and means of prevention," *Postharvest Biology and Technology*, vol. 139, pp. 135–149, 2018. [Online]. Available: <https://www.sciencedirect.com/science/article/pii/S0925521417309559>
37. M. F. Bambace, M. V. Alvarez, and M. del Rosario Moreira, "Novel functional blueberries: Fructo-oligosaccharides and probiotic lactobacilli incorporated into alginate edible coatings," *Food Research International*, vol. 122, pp. 653–660, 2019. [Online]. Available: <https://www.sciencedirect.com/science/article/pii/S0963996919300407>
38. F. Arguello, X. Rojas-Lema, and F. Iza, "Línea base de la calidad de la mora de castilla (*rubus glaucus*) en su cadena alimentaria (quality baseline of the castilla blackberry (*rubus glaucus*) in its food chain)," 09 2016.
39. R. Saltos Espín, M. González Rivera, V. González Rivera, F. Cofre Santos, I. Hidalgo Guerrero, L. García Zambrano, and E. Borja Borja, *Revista de Investigación Talentos*, vol. 7, no. 2, pp. 33 – 45, oct. 2020. [Online]. Available: <https://talentos.ueb.edu.ec/index.php/talentos/article/view/222>
40. M. Cortés Rodríguez, C. Villegas Yépez, J. H. Gil González, and R. Ortega-Toro, "Effect of a multifunctional edible coating based on cassava starch on the shelf life of andean blackberry," *Heliyon*, vol. 6, no. 5, p. e03974, 2020. [Online]. Available: <https://www.sciencedirect.com/science/article/pii/S2405844020308197>
41. V. Siracusa and I. Blanco, "Bio-polyethylene (bio-pe), bio-polypropylene (bio-pp) and bio-poly(ethylene terephthalate) (bio-pet): Recent developments in bio-based polymers analogous to petroleum-derived ones for packaging and engineering applications," *Polymers*, vol. 12, no. 8, 2020. [Online]. Available: <https://www.mdpi.com/2073-4360/12/8/1641>
42. X. Zhong, X. Zhao, Y. Qian, and Y. Zou, "Polyethylene plastic production process," *Insight - Material Science*, vol. 1, p. 1, 08 2018.
43. J. Lee, *Chapter 4. Blackberry fruit quality components, composition, and potential health benefits*, 10 2017, pp. 49–62.
44. L. M. Arbeláez-Arias, J. C. Lucas-Aguirre, and L. G. Gutiérrez-López, "Induction and multiplication of thornless *rubus glaucus* callogenesis from leaves," *Journal of Hunan University Natural Sciences*, vol. 50, no. 10, 2023.
45. J. Fernandez-Salvador, B. C. Strik, Y. Zhao, and C. E. Finn, "Trailing blackberry genotypes differ in yield and postharvest fruit quality during establishment in an organic production system," *HortScience*, vol. 50, no. 2, pp. 240 – 246, 2015. [Online]. Available: <https://journals.ashs.org/hortsci/view/journals/hortsci/50/2/article-p240.xml>
46. I. Samaniego, B. Brito, W. Viera, A. Cabrera, W. Llerena, T. Kannangara, R. Vilcacundo, I. Angós, and W. Carrillo, "Influence of the maturity stage on the phytochemical composition and the antioxidant activity of four andean blackberry cultivars (*rubus glaucus* benth) from ecuador," *Plants*, vol. 9, no. 8, 2020. [Online]. Available: <https://www.mdpi.com/2223-7747/9/8/1027>
47. L. Isaza, Y. P. Zuluaga, and M. L. Marulanda, "Morphological, pathogenic and genetic diversity of *botrytis cinerea* in blackberry cultivations in colombia," *Revista Brasileira de Fruticultura*, vol. 41, no. 6, p. e-490, 2019. [Online]. Available: <https://doi.org/10.1590/0100-29452019490>
48. M. Iza, P. Viteri, M. Hinojosa, A. Martinez, A. Sotomayor, and W. Viera, "Morphological, phenological and pomological differentiation of commercial blackberry (*rubus glaucus* benth.) cultivars," *Trends in Horticulture*, vol. 5, p. 38, 07 2022.
49. A. Alvarez, H. Silva-Rojas, S. Leyva-Mir, N. Marbán-Mendoza, and A. Rebollar-Alviter, "Resistance of *botrytis cinerea* from strawberry (*fragaria x ananassa* duch.) to fungicides in michoacan mexico resistencia de *botrytis cinerea* de fresa (*fragaria x ananassa* duch.) a fungicidas en michoacAn mÉxico," *Agrociencia*, vol. 51, pp. 783–798, 10 2017.
50. P. Boeri, L. Piñuel, D. Dalzotto, R. Monasterio, A. Fontana, S. Sharry, D. A. Barrio, and W. Carrillo, "Argentine patagonia barberry chemical composition and evaluation of its antioxidant capacity," *Journal of*

Food Biochemistry, vol. 44, no. 7, p. e13254, 2020. [Online]. Available: <https://onlinelibrary.wiley.com/doi/abs/10.1111/jfbc.13254>

51. G. X. Galarza, A. Escuela, A. Panamericana, and Z. Honduras, "Efecto de la acción enzimática en la hidrolización de elagitaninos e incremento de ácido elágico en mora, frambuesa y guayaba," 2017. [Online]. Available: <https://bdigital.zamorano.edu/handle/11036/5967>
52. T. María Guzmán, K. Cuenca, and E. Tacuri, "Caracterización de la poscosecha de la mora de castilla (*rubus glaucus*) tratada con 1-metilciclopropeno," *Revista Ciencias Técnicas Agropecuarias*, vol. 27, no. 1, pp. 66–75, 2018.
53. F. Arguello, X. Rojas-Lema, and F. Iza, "Línea base de la calidad de la mora de castilla (*rubus glaucus*) en su cadena alimentaria (quality baseline of the castilla blackberry (*rubus glaucus*) in its food chain)," 09 2016.
54. S. Úbeda Jasanada, M. Aznar, and C. Nerín, "Determinación de oligómeros en ácido poliláctico, pla, biopolímero destinado al envase alimentario," *Jornada de Jóvenes Investigadores del I3A*, vol. 6, 05 2018.
55. M. d. L. R., C. ., and S. ., "Almidón modificado: Propiedades y usos como recubrimientos comestibles para la conservación de frutas y hortalizas frescas," *Revista Iberoamericana de Tecnología Postcosecha*, vol. 19, 2018. [Online]. Available: <https://www.redalyc.org/articulo.oa?id=81355612003>
56. K. Majeed, R. Arjmandi, and A. Hassan, "Mechanical and oxygen barrier properties of ldpe/mmt/mape and ldpe/mmt/eva nanocomposite films: A comparison study," *Journal of Physical Science*, vol. 29, pp. 43–58, 05 2018.
57. M. Riera and I. Campozano, "Ácido poliláctico: una revisión de los métodos de producción y sus aplicaciones," *Publicaciones en Ciencias y Tecnología*, vol. 16, pp. 42–53, 07 2022.
58. S. Kormin, F. Kormin, M. D. H. Beg, and M. B. M. Piah, "Physical and mechanical properties of ldpe incorporated with different starch sources," *IOP Conference Series: Materials Science and Engineering*, vol. 226, no. 1, p. 012157, aug 2017. [Online]. Available: <https://dx.doi.org/10.1088/1757-899X/226/1/012157>
59. S. Ospina and J. Cartagena, "Modified atmosphere: an alternative for food preservation," *Revista Lasallista de Investigación*, vol. 5, pp. 112–123, 07 2008.
60. S. Bertin and J.-J. Robin, "Study and characterization of virgin and recycled ldpe/pp blends," *European Polymer Journal*, vol. 38, no. 11, pp. 2255–2264, 2002. [Online]. Available: <https://www.sciencedirect.com/science/article/pii/S0014305702001118>
61. D. M. Hernández Pachón, S. M. Árdila Panesso, J. S. Díaz Jiménez, M. A. Perilla Gómez, D. D. Cubillos Pedraza, J. C. Serrano Sánchez, M. F. Quesada Pacheco, and N. L. Pulido Ortíz, "Caracterización de agentes causales de enfermedades en el cultivo de mora (*Rubus glaucus*) en la finca manantial en la vereda sabaneta, municipio de La Vega, Cundinamarca," *Revista Ciencias Agropecuarias (RCA)*, ISSN-e 2422-3484, Vol. 4, N^o. 1, 2018, págs. 9-17, vol. 4, no. 1, pp. 9–17, 2018.
62. M. A. Mora-Ramos, F. P. Pardo-Carrasco, and H. Bastidas-López, "Diagnóstico patológico en mora de castilla *rubus glaucus* bentham (*rosales:rosaceae*)," *ORINOQUIA*, vol. 24, pp. 27 – 32, 12 2020. [Online]. Available: <http://www.scielo.org.co/scielo.php?script=sci.arttext&pid=S0121-37092020000200027&nrm=iso>

License

Copyright (2024) © Eduardo Teneda-Ramos, Lorena Cáceres-Miranda, Pedro Escudero-Villa, Esteban Fuentes-Pérez and José Varela-Aldás.

This text is protected under an international Creative Commons 4.0 license.



You are free to share, copy, and redistribute the material in any medium or format — and adapt the document — remix, transform, and build upon the material — for any purpose, even commercially, provided you comply with the conditions of Attribution. You must give appropriate credit to the original work, provide a link to the license, and indicate if changes were made. You may do so in any reasonable manner, but not in a way that suggests endorsement by the licensor or approval of your use of the work.

License summary - Full text of the license

PI-Filter compensator for LQG controller aimed to fixed-wings aircrafts

María del Carmen Claudio · Alida Ortíz-Pupo · Gloria Chicaiza-Claudio

Received: 13 January 2024 / Accepted: 10 May 2024 / Published: 15 May 2024

Abstract: Fixed-wing aircraft generate lift and propulsion using their wings, relying on forward motion for airflow instead of rotating blades like helicopters. They offer advantages such as extended range, higher velocities, stability in turbulent weather, and lower operational costs compared to rotary-wing aircraft. This study introduces a method to enhance control smoothness for fixed-wing aircraft using Linear Quadratic Gaussian control and Proportional-Integral filter compensation. Flight simulators like FlightGear are employed to test control algorithms, providing realistic flight dynamics and versatile options for various aircraft types. This approach offers a cost-effective and efficient means to develop and test controllers for challenging flight scenarios, while demonstrating the performance of the LQG+PI method by displaying the trends in longitudinal and lateral control errors.

Keywords PI+LQG · fixed-wing aircraft · FlightGear


1 Introduction

Fixed-wing aircraft are airplanes that generate lift and propulsion by directing airflow over their wings, which remain fixed in position during flight [1]. Unlike rotorcraft such as helicopters, which utilize rotating wings or blades to achieve lift, fixed-wing aircraft rely on forward motion to create the airflow necessary for lift generation. While rotary-wing aircraft offer enhanced maneuverability due to their ability to perform vertical takeoff and hovering, fixed-wing aircraft are the standard in aviation for various purposes, including long-distance

transportation, aerial surveillance, cargo transport, and military operations [2]. This preference is due to the inherent advantages rooted in the aerodynamic design and operational characteristics. The advantages of fixed-wing aircraft are numerous and encompass various aspects of performance, efficiency, versatility, and operational capability. Compared to rotary-wing aircraft, fixed-wing types offer extended flight range and endurance due to their design optimized for forward motion rather than vertical takeoff and hovering [3]. Additionally, fixed-wing aircraft can achieve significantly higher speeds, thanks to their aerodynamic configuration, and they demonstrate superior stability in turbulent weather conditions [4]. Moreover, fixed-wing aircraft can carry larger payloads and offer lower operational and maintenance costs than rotary-wing aircraft.

Flight simulators are a cost-effective and efficient way to calibrate, test, and improve control algorithms before conducting experiments on fixed-wing aircraft. Whether for military, entertainment, or commercial applications, a suitable simulator can be an excellent tool for proper vehicle handling, particularly when the vehicle can be damaged if the pilot loses control or is inexperienced [5]. In this context, the control of an aircraft that is challenging to test in a laboratory can be significantly enhanced by utilizing a simulator with flexible characteristics capable of interfacing with mathematical software, especially when assessing responses to wind disturbances that are difficult to measure and replicate experimentally. Simulation software such as X-Plane, AirSim, Gazebo, and FlightGear have such capabilities, with research studies employing them for various purposes. FlightGear features an intuitive user interface, the ability to communicate with external software, dynamic properties for an assortment of freely downloadable simulated prototypes, options for adding a debugging mode for communication errors, and the ability to display prototype states over LAN networks [6]. Furthermore, the versatility of FlightGear allows the use of different aircraft and flying objects and avoids the use of potentially oversimplified flight dynamics mod-

María del Carmen Claudio  · Gloria Chicaiza-Claudio 
Inmersoft Technologies
Quito, Ecuador
{mclaudio, gchicaiza}@inmersoft.com

Alida Ortíz-Pupo 
Instituto de Automática
Universidad Nacional de San Juan
San Juan, Argentina
aortiz@inaut.unsj.edu.ar

els. Given these features, FlightGear can communicate with mathematical software to modify the state of simulated prototype actuators to test controllers or calibrate them against simulated disturbances [7]. In this way, FlightGear performs the flight calculations, with the program treated as a black box to Matlab, akin to a real aircraft [8]. This approach leverages a high degree of realism provided by FlightGear, which utilizes established and realistic Flight Dynamics Models (FDMs) [9] based on nonlinear equations of motion.

Research has explored the use of LQG control for managing fixed-wing aircraft [10], yet a significant hurdle emerges during the linearization process and the dynamic alteration of linearization points, leading to unwanted abrupt maneuvers [11]. To overcome this challenge, this study introduces a PI filter compensation method aimed at enhancing the smoothness of LQG-generated control. As the aircraft, we used the F-104 Starfighter data to achieve the linearized model while employing its complete dynamics within FlightGear. The results show the lateral and longitudinal behavior of the system, indicating a trend of control errors towards zero.

The article is divided into five parts, including the Introduction and Conclusions. In Section 2, the linearization of the model is presented, while Section 3 develops the PI-Filter compensator. Furthermore, Section 4 includes the results of this work.

2 Modeling

When determining the acceleration of each mass element, we must consider the contributions to its velocity from both the linear velocities (u, v, w) in each of the coordinate directions and the contributions due to the rotational rates (p, q, r) about the axes (Fig. 1). Therefore, the time rates of change of the coordinates in an inertial frame that is instantaneously coincident with the body axes are:

$$\begin{aligned}\dot{x} &= u + qz - ry, \\ \dot{y} &= v + rx - pz, \\ \dot{z} &= w + py - qx.\end{aligned}$$

The linearized equations are derived from Caughey et al. [12]. In this way, for the longitudinal control, the equation is given by:

$$\begin{bmatrix} \dot{u} \\ \dot{\omega} \\ \dot{q} \\ \dot{\theta} \end{bmatrix} = \mathbf{F}_{\text{LO}} \begin{bmatrix} u \\ \omega \\ q \\ \theta \end{bmatrix} + \mathbf{G}_{\text{LO}} \begin{bmatrix} \delta_e \\ \delta_T \end{bmatrix}, \quad (1)$$

where

$$\mathbf{F}_{\text{LO}} = \begin{bmatrix} X_u & X_\omega & 0 & -g \\ Z_u & Z_\omega & u_0 & 0 \\ M_u + M_{\dot{\omega}}Z_u & M_\omega + M_{\dot{\omega}}Z_\omega & M_q + M_{\dot{\omega}}u_0 & 0 \\ 0 & 0 & 1 & 0 \end{bmatrix}, \quad (2)$$

and

$$\mathbf{G}_{\text{LO}} = \begin{bmatrix} X_e & X_T \\ Z_e & Z_T \\ M_e + M_{\dot{\omega}}Z_e & M_T + M_{\dot{\omega}}Z_T \\ 0 & 0 \end{bmatrix}. \quad (3)$$

Here, the state vector is $\mathbf{x}_{\text{LO}} = [u \ \omega \ q \ \theta]^T$ and the longitudinal control vector (elevator and throttle) is $\eta = [\delta_e \ \delta_T]^T$. The orientation of the body is determined by (β, θ, ϕ) , with β representing the yaw rotation about the Z-axis, θ the pitch rotation about the Y-axis, and ϕ the roll rotation about the X-axis.

On the other hand, the equation for the lateral control is:

$$\begin{bmatrix} \dot{\beta} \\ \dot{p} \\ \dot{r} \\ \dot{\phi} \end{bmatrix} = \mathbf{F}_{\text{LA}} \begin{bmatrix} \beta \\ p \\ r \\ \phi \end{bmatrix} + \mathbf{G}_{\text{LA}} \begin{bmatrix} \delta_a \\ \delta_r \end{bmatrix}, \quad (4)$$

where

$$\mathbf{F}_{\text{LA}} = \begin{bmatrix} Y_\beta/u_0 & Y_p/u_0 & -(1 - Y_r/u_0) & -g/u_0 \\ L_\beta & L_p & L_r & 0 \\ N_\beta & N_p & N_r & 0 \\ 0 & 1 & 0 & 0 \end{bmatrix}, \quad (5)$$

and

$$\mathbf{G}_{\text{LA}} = \begin{bmatrix} 0 & Y_r/u_0 \\ L_a & L_r \\ N_a & N_r \\ 0 & 0 \end{bmatrix}. \quad (6)$$

Here, the state vector is $\mathbf{x}_{\text{LA}} = [\beta \ p \ r \ \phi]^T$ and the lateral control vector (aileron and rudder) is $\eta = [\delta_a \ \delta_r]^T$.

3 PI-Filter compensation

The non-zero point regulator is designed under the assumption that the system to be controlled is modeled without error and that any system disturbances are white random processes. However these conditions are violated because of slowly varying disturbances of uncertain magnitude, that makes the basic LQ regulation inadequate. Therefore there is the need to increase system robustness by providing dynamic compensation

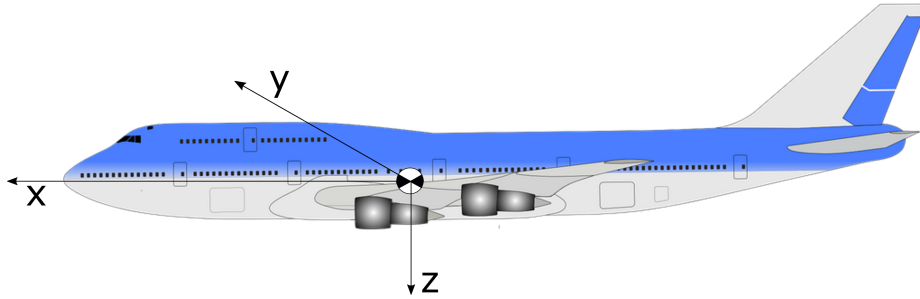


Fig. 1 The body axis system is centered at the center of gravity of the flight vehicle. The y-axis extends out towards the right wing.

which can be accomplished by adding new states to the closed-loop system. The state vector is augmented, corresponding differential equations are added to the system model and the control law that minimizes a quadratic cost function is computed for the augmented systems. In particular the proportional-integral compensation introduces command-error integrals to the LQ control law. The systems to be controlled is described by the linear, time-invariant model

$$\dot{\mathbf{x}}(t) = \mathbf{F}\mathbf{x}(t) + \mathbf{G}\mathbf{u}(t) + \mathbf{L}\mathbf{w}(t),$$

$$\mathbf{y}(t) = \mathbf{H}_x\mathbf{x}(t) + \mathbf{H}_u\mathbf{u}(t) + \mathbf{H}_w\mathbf{w}(t).$$

It is assumed that \mathbf{F} , \mathbf{G} , \mathbf{H}_x , \mathbf{H}_u , \mathbf{L} , and \mathbf{H}_w are known without error and are a generalization of the lateral and longitudinal linearization.

The equilibrium of the system is reached when $\dot{\mathbf{x}}(t) = \mathbf{0}$. Therefore, we can represent the state system equations as follows

$$\begin{bmatrix} \mathbf{0} \\ \mathbf{y}^* \end{bmatrix} = \begin{bmatrix} \mathbf{F} & \mathbf{G} \\ \mathbf{H}_x & \mathbf{H}_u \end{bmatrix} \begin{bmatrix} \mathbf{x}^* \\ \mathbf{u}^* \end{bmatrix} + \begin{bmatrix} \mathbf{L} \\ \mathbf{H}_w \end{bmatrix} \mathbf{w}^*,$$

which can also be written as

$$\begin{bmatrix} \mathbf{0} - \mathbf{L}\mathbf{w}^* \\ \mathbf{y}^* - \mathbf{H}_w\mathbf{w}^* \end{bmatrix} = \begin{bmatrix} \mathbf{F} & \mathbf{G} \\ \mathbf{H}_x & \mathbf{H}_u \end{bmatrix} \begin{bmatrix} \mathbf{x}^* \\ \mathbf{u}^* \end{bmatrix}.$$

If the variables \mathbf{x}^* and \mathbf{u}^* are solved, then:

$$\begin{bmatrix} \mathbf{x}^* \\ \mathbf{u}^* \end{bmatrix} = \begin{bmatrix} \mathbf{F} & \mathbf{G} \\ \mathbf{H}_x & \mathbf{H}_u \end{bmatrix}^{-1} \begin{bmatrix} \mathbf{0} - \mathbf{L}\mathbf{w}^* \\ \mathbf{y}^* - \mathbf{H}_w\mathbf{w}^* \end{bmatrix}. \quad (7)$$

Let's define:

$$\mathbf{A} = \begin{bmatrix} \mathbf{F} & \mathbf{G} \\ \mathbf{H}_x & \mathbf{H}_u \end{bmatrix}$$

and

$$\mathbf{B} = \begin{bmatrix} \mathbf{B}_{11} & \mathbf{B}_{12} \\ \mathbf{B}_{21} & \mathbf{B}_{22} \end{bmatrix} = \mathbf{A}^{-1};$$

then, the equation (7) can be written as:

$$\begin{bmatrix} \mathbf{x}^* \\ \mathbf{u}^* \end{bmatrix} = \begin{bmatrix} \mathbf{B}_{11} & \mathbf{B}_{12} \\ \mathbf{B}_{21} & \mathbf{B}_{22} \end{bmatrix} \begin{bmatrix} \mathbf{0} - \mathbf{L}\mathbf{w}^* \\ \mathbf{y}^* - \mathbf{H}_w\mathbf{w}^* \end{bmatrix}.$$

The reference values \mathbf{x}^* and \mathbf{u}^* , dependent on the desired input \mathbf{y}^* (Fig. 2), are

$$\mathbf{x}^* = -\mathbf{B}_{11}\mathbf{L}\mathbf{w}^* + \mathbf{B}_{12}(\mathbf{y}^* - \mathbf{H}_w\mathbf{w}^*),$$

$$\mathbf{u}^* = -\mathbf{B}_{21}\mathbf{L}\mathbf{w}^* + \mathbf{B}_{22}(\mathbf{y}^* - \mathbf{H}_w\mathbf{w}^*);$$

with

$$\mathbf{B}_{11} = \mathbf{F}^{-1}(-\mathbf{G}\mathbf{B}_{21} + \mathbf{I}_n),$$

$$\mathbf{B}_{12} = -\mathbf{F}^{-1}\mathbf{G}\mathbf{B}_{22},$$

$$\mathbf{B}_{21} = -\mathbf{B}_{22}\mathbf{H}_x\mathbf{F}^{-1},$$

$$\mathbf{B}_{22} = (-\mathbf{H}_x\mathbf{F}^{-1}\mathbf{G} + \mathbf{H}_u)^{-1}.$$

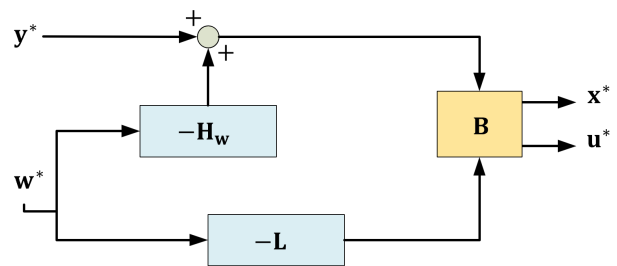


Fig. 2 Reference values depending on the desired inputs

The quadratic cost function for the Proportional-Integral-Filter Compensation is

$$J = \lim_{T \rightarrow \infty} \frac{1}{2T} \int_0^T \left\{ \begin{bmatrix} \tilde{\mathbf{x}}^T(t) & \tilde{\mathbf{u}}^T(t) & \xi^T(t) \end{bmatrix} \Gamma \begin{bmatrix} \tilde{\mathbf{x}}(t) \\ \tilde{\mathbf{u}}(t) \\ \xi(t) \end{bmatrix} + \mathbf{v}^T(t) \mathbf{R}_2 \mathbf{v}(t) \right\} dt, \quad (8)$$

with

$$\Gamma = \begin{bmatrix} \mathbf{Q}_1 & \mathbf{M} & \mathbf{0} \\ \mathbf{M}^T & \mathbf{R}_1 & \mathbf{0} \\ \mathbf{0} & \mathbf{0} & \mathbf{Q}_2 \end{bmatrix},$$

where \mathbf{R}_1 , \mathbf{M} , \mathbf{Q}_1 , and \mathbf{Q}_2 are gain matrices.

This equation may be reformulated considering

$$\dot{\tilde{\mathbf{x}}}(t) = \mathbf{F}\tilde{\mathbf{x}}(t) + \mathbf{G}\tilde{\mathbf{u}}(t),$$

$$\dot{\tilde{\mathbf{u}}}(t) = \dot{\mathbf{u}}_C(t) \triangleq \mathbf{v}(t),$$

and adding the integral-state vector to this, the augmented state equation can be formed

$$\begin{bmatrix} \dot{\tilde{\mathbf{x}}}(t) \\ \dot{\tilde{\mathbf{u}}}(t) \\ \dot{\xi}(t) \end{bmatrix} = \begin{bmatrix} \mathbf{F} & \mathbf{G} & \mathbf{0} \\ \mathbf{0} & \mathbf{0} & \mathbf{0} \\ \mathbf{H}_x & \mathbf{H}_u & \mathbf{0} \end{bmatrix} \begin{bmatrix} \tilde{\mathbf{x}}(t) \\ \tilde{\mathbf{u}}(t) \\ \xi(t) \end{bmatrix} + \begin{bmatrix} \mathbf{0} \\ \mathbf{I}_m \\ \mathbf{0} \end{bmatrix} \mathbf{v}(t); \quad (9)$$

where

$$\tilde{\mathbf{u}}(t) = \mathbf{u}(t) - \mathbf{u}^*,$$

$$\tilde{\mathbf{x}}(t) = \mathbf{x}(t) - \mathbf{x}^*,$$

$$\xi(t) = \xi(0) + \int_0^t (\mathbf{y}(\tau) - \mathbf{y}^*) d\tau.$$

The augmented state equation (9) can also be written as

$$[\dot{\chi}(t)] = \begin{bmatrix} \mathbf{F} & \mathbf{G} & \mathbf{0} \\ \mathbf{0} & \mathbf{0} & \mathbf{0} \\ \mathbf{H}_x & \mathbf{H}_u & \mathbf{0} \end{bmatrix} \chi(t) + \begin{bmatrix} \mathbf{0} \\ \mathbf{I}_m \\ \mathbf{0} \end{bmatrix} \mathbf{v}(t),$$

with

$$\chi(t) \triangleq \begin{bmatrix} \tilde{\mathbf{x}}(t) \\ \tilde{\mathbf{u}}(t) \\ \xi(t) \end{bmatrix}.$$

The cost function in (8) then becomes

$$J = \lim_{T \rightarrow \infty} \frac{1}{2T} \int_0^T [\chi^T(t) \mathbf{Q}' \chi(t) + \mathbf{v}^T(t) \mathbf{R}' \mathbf{v}(t)] dt,$$

which leads to a control law of the form

$$\mathbf{v}(t) = -\mathbf{C}\chi(t)$$

or

$$\mathbf{v}(t) = -\mathbf{C}_1 \tilde{\mathbf{x}}(t) - \mathbf{C}_2 \tilde{\mathbf{u}}(t) - \mathbf{C}_3 \xi(t).$$

This equation is equivalent to

$$\dot{\mathbf{u}}(t) = -\mathbf{C}_1 [\mathbf{x}(t) - \mathbf{x}^*] - \mathbf{C}_2 [\mathbf{u}(t) - \mathbf{u}^*] - \mathbf{C}_3 \left\{ \xi(0) + \int_0^t (\mathbf{y}(\tau) - \mathbf{y}^*) d\tau \right\}, \quad (10)$$

with

$$\mathbf{y}^* = \mathbf{H}_x \mathbf{x}^* + \mathbf{H}_u \mathbf{u}^*.$$

The control law (10) can be rearranged as

$$\dot{\mathbf{u}}(t) = (\mathbf{C}_1 \mathbf{B}_{12} + \mathbf{C}_2 \mathbf{B}_{22}) \mathbf{y}^* - \mathbf{C}_1 \mathbf{x}(t) - \mathbf{C}_2 \mathbf{u}(t) - \mathbf{C}_3 \left\{ \xi(0) + \int_0^t (\mathbf{y}(\tau) - \mathbf{y}^*) d\tau \right\} \quad (11)$$

and

$$\dot{\mathbf{u}}(t) = \mathbf{C}_F \mathbf{y}^* - \mathbf{C}_B \mathbf{x}(t) - \mathbf{C}_C \mathbf{u}(t) - \mathbf{C}_I \left\{ \xi(0) + \int_0^t (\mathbf{y}(\tau) - \mathbf{y}^*) d\tau \right\}, \quad (12)$$

with $\mathbf{C}_F = \mathbf{B}_{22} + \mathbf{C}_1 \mathbf{B}_{12}$, $\mathbf{C}_B = \mathbf{C}_1$, $\mathbf{C}_C = \mathbf{C}_2$, $\mathbf{C}_I = \mathbf{C}_3$.

The implementation of the complete controller is visualized in Fig. 3, where the connection of the control outputs to FlightGear is shown, with the matrix calculations being performed in Matlab.

4 Results

4.1 Intercommunication

Based on the work of Aschauer et al. [13], we have programmed a UDP-based communication tunnel to exchange information between the mathematical software and the flight simulator (see Fig. 5) through an information frame. The parameters for obtaining the linearized model are taken from:

F-104 Starfighter parameters

<http://www.gnu-darwin.org/ProgramDocuments/f104/linear.html>

Additionally, the software is executed with the following command:

Command to execute FlightGear

```
C:\ProgramFiles\FlightGear_2017.3.1\bin\fgfs
-aircraft=F-104
-start-date-lat=2004:06:01:09:00:00
-generic=
-socket,out,20,localhost,2054,udp,readUDP
-generic=
-socket,in,20,localhost,2055,udp,writeUDP
```

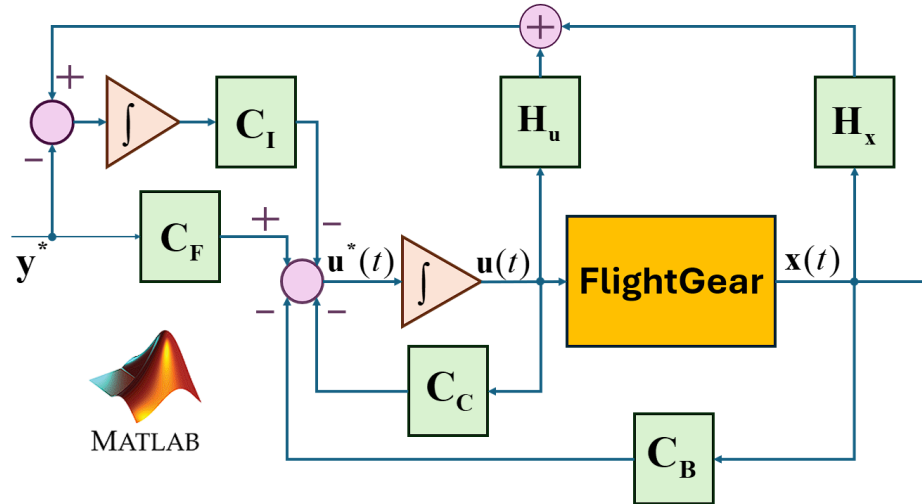


Fig. 3 Proportional-integral (PI) regulator for nonsingular command vector

where the aircraft type is specified (in our case, the F-104 Starfighter), along with the simulation start date and time, and the UDP ports for information exchange. Finally, the controllers defined in Section 3 are programmed in Simulink, as shown in Fig. 4.

4.2 States and control errors

The intercommunication between programs allows reading the states of the simulated aircraft in Matlab, while the control actions are reflected in FlightGear. Thus, we plot all states of both longitudinal and lateral behavior in Figures 6 and 7, respectively. For the longitudinal behavior, we assume a constant throttle, while setting an elevation of 20 degrees, starting from an initial elevation of -20 degrees. On the other hand, for the lateral behavior, both pitch and roll need to be controlled. Therefore, the roll starts from an angle of 5 degrees, with a desired roll of 20 degrees. Similarly, the pitch starts from an angle of 10 degrees and needs to reach 5 degrees. Both Figure 6 and Figure 7 demonstrate the trend of errors approaching zero.

5 Conclusions

In conclusion, this study focuses on the development and implementation of control techniques for fixed-wing aircraft, leveraging flight simulators as a primary tool for algorithm validation and testing. Key methodologies such as LQG control and PI filter compensation are employed to enhance control smoothness and efficiency. The integration of UDP-based communication tunnels facilitates seamless data exchange between the

flight simulator and mathematical software like Matlab, crucial for real-time control and simulation. Results presented demonstrate the longitudinal and lateral behavior of the controlled system, indicating a trend towards minimal control errors.

Appendix: Tables with constants required for linearization

Table 1 Constants for Longitudinal-Directional System

Parameter	Value
Stability Derivative	$X_u = -0.0093$
Angle of Attack Deriv.	$X_w = -0.0253$
Stability Derivative	$Z_u = -0.0236$
Angle of Attack Derivative	$Z_w = -0.1982$
Gravity in Slugs	$g = 32.174$
Initial vel.	$u_0 = 1740.81$
Compressibility Effect Deriv.	$M_u = 0.0$
Elev. Deflection	$X_e = 0.0$
Dimensional Pitching Mom. Deriv.	$M_w = -0.0104$
Dimensional Pitching Mom. Deriv.	$M_{\dot{w}} = 0.0$
Dimensionless Pitching Mom. Deriv.	$M_q = -0.1845$
Thrust Deflection	$X_T = 0$
Thrust Deflection	$Z_T = 0$
Pitching Mom. (Thrust Deflection)	$M_T = 0$
Pitching Mom. (Elevator Deflection)	$M_e = -18.1525$
Elevator Deflection	$Z_e = -87.9155$

Conflict of interest

The authors declare that they have no conflict of interest.

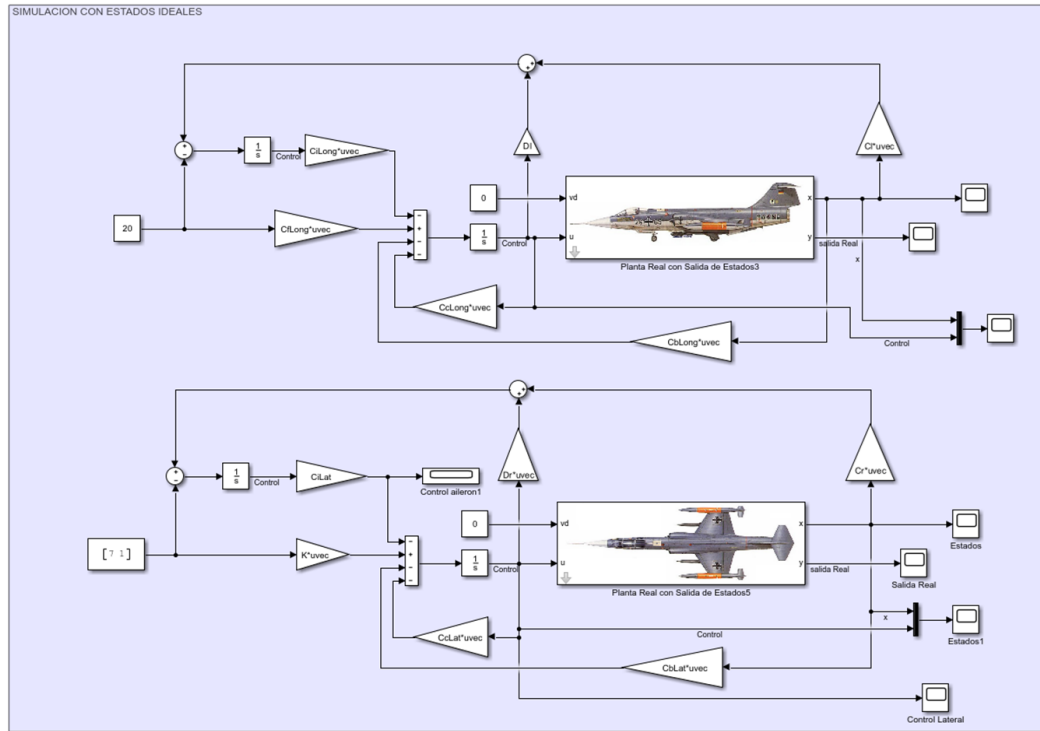


Fig. 4 Programming of the controller in Simulink

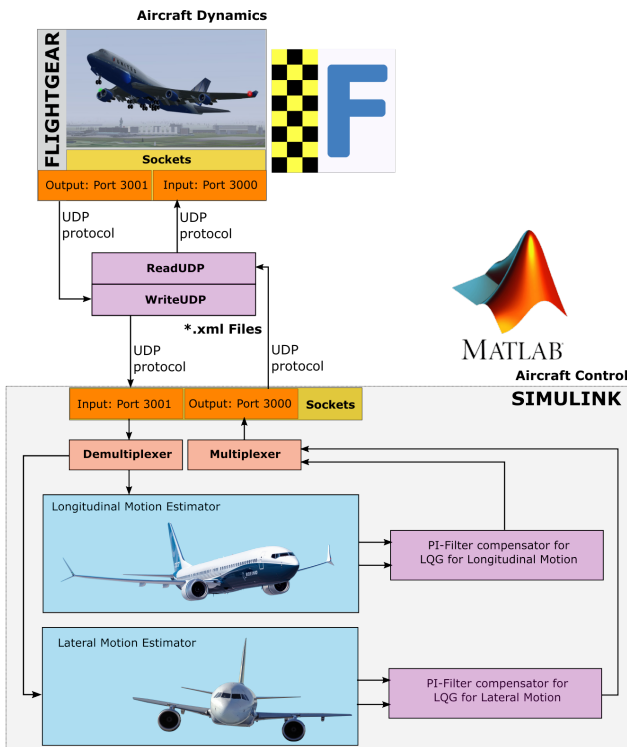


Fig. 5 Connection between Matlab and FlightGear

References

1. B. Sarlioglu and C. T. Morris, “More electric aircraft: Review, challenges, and opportunities for commercial

Table 2 Constants for Lateral–Directional System

Parameter	Value
Roll Rate	$Y_p = 0.0$
Sideslip Derivative	$Y_\beta = -175.6628$
Yaw Rate Derivative	$Y_r = 0$
Aileron Deflection Derivative	$Y_a = 0$
Rolling Moment	$L_p = -0.8864$
Rolling Moment	$L_r = 4.0927$
Rolling Moment	$L_a = -63.6874$
Roll Acceleration	$L_\beta = -48.1804$
Yawing Moment	$N_a = -0.0777$
Yawing Moment	$N_p = -0.0182$
Yawing Moment	$N_r = -1.3522$
Yaw Acceleration	$N_\beta = 7.5224$

transport aircraft,” *IEEE transactions on Transportation Electrification*, vol. 1, no. 1, pp. 54–64, 2015.

2. S. G. Gupta, D. M. Ghonge, and P. M. Jawandhiya, “Review of unmanned aircraft system (uas),” *International Journal of Advanced Research in Computer Engineering & Technology (IJARCET) Volume*, vol. 2, 2013.

3. B. J. Brelje and J. R. Martins, “Electric, hybrid, and turboelectric fixed-wing aircraft: A review of concepts, models, and design approaches,” *Progress in Aerospace Sciences*, vol. 104, pp. 1–19, 2019.

4. D. B. Barber, J. D. Redding, T. W. McLain, R. W. Beard, and C. N. Taylor, “Vision-based target geo-location using a fixed-wing miniature air vehicle,” *Journal of Intelligent and Robotic Systems*, vol. 47, pp. 361–382, 2006.

5. J. Veltman, “A comparative study of psychophysiological reactions during simulator and real flight,” *The Interna-*

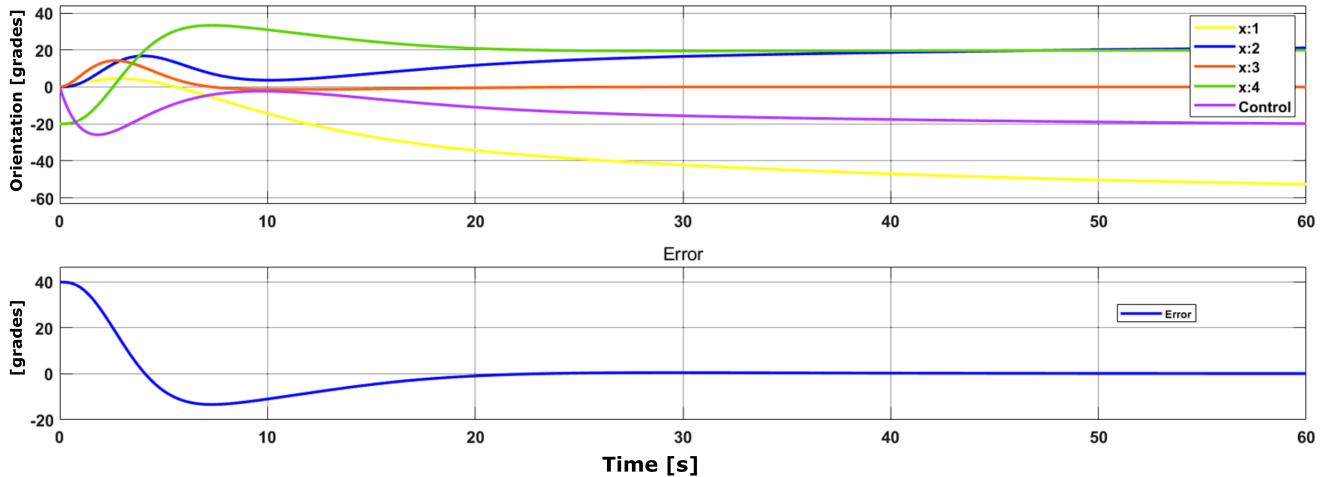


Fig. 6 Longitudinal states values and control error

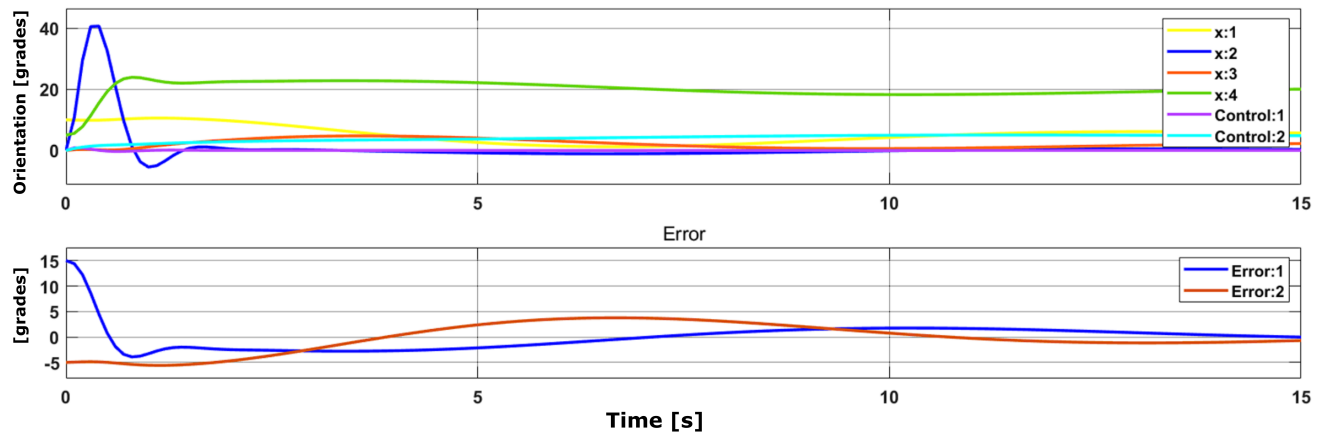


Fig. 7 Lateral states values and control errors

- tional Journal of Aviation Psychology*, vol. 12, no. 1, pp. 33–48, 2002.
6. A. Nisansala, M. Weerasinghe, G. Dias, D. Sandaruwan, C. Keppitiyagama, N. Kodikara, C. Perera, and P. Samarasinghe, “Flight simulator for serious gaming,” in *Information Science and Applications*. Springer, 2015, pp. 267–277.
 7. J. Ying, H. Luc, J. Dai, and H. Pan, “Visual flight simulation system based on matlab/flightgear,” in *2017 IEEE 2nd Advanced Information Technology, Electronic and Automation Control Conference (IAEAC)*. IEEE, 2017, pp. 2360–2363.
 8. N. Horri and M. Pietraszko, “A tutorial and review on flight control co-simulation using matlab/simulink and flight simulators,” *Automation*, vol. 3, no. 3, pp. 486–510, 2022.
 9. A. I. Hentati, L. Krichen, M. Fourati, and L. C. Fourati, “Simulation tools, environments and frameworks for uav systems performance analysis,” in *2018 14th International Wireless Communications & Mobile Computing Conference (IWCMC)*. IEEE, 2018, pp. 1495–1500.
 10. E. N. Demirhan, K. Ç. Coşkun, and C. Kasnaoğlu, “Lqı control design with lqg regulator via ukf for a fixed-wing aircraft,” in *2020 24th International Conference on System Theory, Control and Computing (ICSTCC)*. IEEE, 2020, pp. 25–30.
 11. S. G. Clarke and I. Hwang, “Deep reinforcement learning control for aerobatic maneuvering of agile fixed-wing aircraft,” in *AIAA Scitech 2020 Forum*, 2020, p. 0136.
 12. D. A. Caughey, “Introduction to aircraft stability and control course notes for m&ae 5070,” *Sibley School of Mechanical & Aerospace Engineering Cornell University*, vol. 15, 2011.
 13. G. Aschauer, A. Schirrer, and M. Kozek, “Co-simulation of matlab and flightgear for identification and control of aircraft,” *IFAC-PapersOnLine*, vol. 48, no. 1, pp. 67–72, 2015.

License

Copyright (2024) © María del Carmen Claudio, Alida Ortiz, Gloria Chicaiza-Claudio.

This text is protected under an international Creative Commons 4.0 license.



You are free to share, copy, and redistribute the material in any medium or format — and adapt the document — remix, transform, and build upon the material — for any purpose, even commercially, provided you comply with the conditions of Attribution. You must give appropriate credit to the original work, provide a link to the license, and indicate if changes were made. You may do so in any reasonable manner, but not in a way that suggests endorsement by the licensor or approval of your use of the work.

License summary - Full text of the license

Real Time Brain Signals Viewer

Celis Gregory · Washington X. Quevedo

Received: 7 January 2024 / Accepted: 2 May 2024 / Published: 14 May 2024

Abstract: This paper addresses the successful integration of Emotiv EPOC and Unity for real-time visualization of brain signals, representing a significant advance in understanding and interacting with brain activity. Real-time visualization of brain signals offers fundamental opportunities in neuroscience, brain-computer interface, and cognitive therapy. Through this study, a solid methodology was established to acquire, process, and graphically represent brain signals in 2D, allowing for an immersive and research-based experience. The results, products generated and implications in areas such as BCI and cognitive therapy are presented. Additionally, future exploration of integration with virtual reality and clinical validation is proposed to advance the understanding and application of real-time brain activity. This research lays the foundation for low-cost research and applications, promoting a deeper understanding of the human mind and its interaction with technology.

Keywords Brain signals · 2D visualization · Real time signals · emotiv-epoc · Unity

1 Introduction

Visualizing brain signals in real time is a fundamental tool in neuroscience and cognitive research [1]. It enables a deeper understanding of brain activity in various situations and contexts, opening possibilities for clinical, research and brain-computer interface (BCI) applications [2]. Brain wave analysis provides crucial information about an individual's mental, emotional,


and cognitive state [3]. The real-time study and visualization of these brain waves has become more accessible thanks to technological advancement, including devices such as Emotiv EPOC [4], which captures non-invasive brain signals. This article focuses on the integration of Emotiv EPOC and Unity, a game-engine, for real-time visualization of brain waves and exploring its possible applications [5].

Below is a review of the literature that supports the importance and relevance of this research. Real-time visualization of brain signals is crucial for understanding brain function, both under normal and pathological conditions. It allows you to identify complex patterns and correlations that would otherwise be difficult to perceive [6]. The visual interpretation of brain activity can help understand cognitive [7], emotional, and decision-making processes. In clinical studies, real-time brain wave visualization is used for monitoring and diagnosing brain disorders such as epilepsy, attention, and hyperactivity disorders (ADHD) [8], and dementia. Additionally, in BCI environments [9], real-time visualization facilitates interaction between the brain and external devices, allowing control of wheelchairs, prostheses, and other devices [10]. The goal of this research is to address the need to build a replicable system that allows real-time visualization of brain waves using Emotiv EPOC and Unity. The aim is to develop a technical solution that provides an intuitive, real-time graphical representation of brain activity, paving the way for future research and interactive applications. The integration of devices like Emotiv EPOC and development environments like Unity represents a significant opportunity to advance this area and develop innovative applications.

2 Problem

Real-time brain wave visualization is an essential tool for understanding the functioning of the human brain [10]. Traditionally, obtaining and analyzing brain signals were complex and expensive processes, reserved

Celis Gregory
BAGO
Quito, Ecuador
gcelis@bago.com.ec

Washington X. Quevedo 
Inmersoft Technologies
Quito, Ecuador
wxquevedo@inmersoft.com

primarily for laboratory environments. However, with the advent of devices such as Emotiv EPOC, which offer more affordable and non-invasive access to brain activity, it has become possible to explore new applications and approaches [11].

Despite advances in technology accessibility, there is still a lack of replicable systems that integrate electronic devices like Emotiv EPOC with development environments like Unity for real-time visualization of brain waves. The scientific community and developers face the challenge of building effective and standardized systems that allow this integration in an effective and easily reproducible way.

The lack of a standardized solution limits progress in research and practical applications. Creating a replicable system, as proposed in this research, is crucial to address this gap and facilitate future advances in neuroscience, BCI, psychology, and other related disciplines. This research is justified by the need to advance in the field of visualization of brain signals in real time and its practical application. The integration of Emotiv EPOC and Unity [12] offers significant potential to explore new frontiers in areas such as cognitive therapy, brain-computer interfaces, brain training and virtual reality.

A replicable solution that allows brain waves to be visualized in real time is an essential step towards more interactive and impactful applications. The development of this solution could lead to significant advances in the design of technologies that improve the quality of life of people with disabilities, allowing communication and interaction with the environment more effectively. Additionally, it could foster education and public understanding of the human brain and its processes.

3 Proposal

The proposed solution is presented in two block diagrams. The first diagram explains the development process from data acquisition to export and subsequent reading. While the second diagram shows the operation of the solution expressed in programming modules with a vision by functions (Fig. 1).

For the development, starting points have been taken from two different points: the origin of the data and the processing of the information received to visualize them numerically and as linear signals in 2D. From the data source we have the Emotiv EPOC device module, which starts with the connection and installation of the manufacturer's own drivers and launchers, to move on to the calibration part since a test user is required to obtain signals. It is necessary to place the sensors in contact

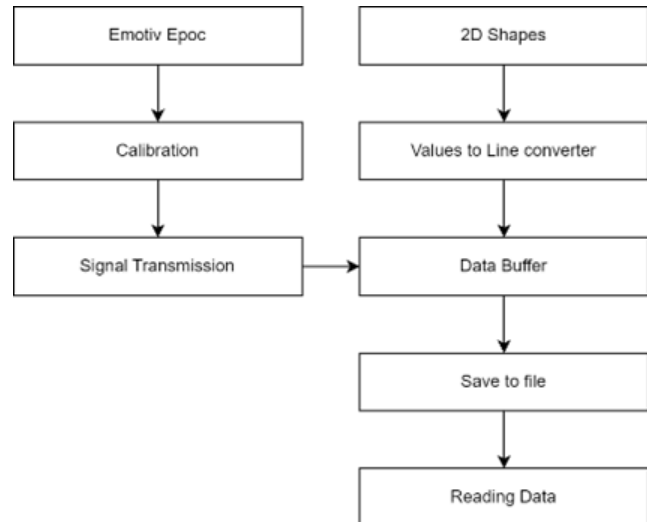


Fig. 1 Diagram of develop path.

with the scalp and add enough output solution to the sensors. In the Signal transmission block, the connection and data transmission are verified in real time from the manufacturer's own hub called Emotiv Launcher. On the other hand, from the game-engine environment, we start from the development of 2D Shapes that will represent the lines with the values of each signal that reaches the environment. This is achieved given that there is a coordinate system with amplitude on the Y axis and time units on the X axis. The location of the values in this Cartesian plane is the function of the block for transforming values into 2D lines. Next, the Data Buffer block is responsible for managing the data that arrives in real time, placing it in temporary memory, keeping it available for representation or storage.

Precisely the save to file block performs the task of storing the displayed data, not the received data, since in the user interface you can modify the time scale values or add marks, in this way the data that the user previously configured, the saving formats are in .CSV and .JSON which may be used by third parties or displayed again differently in a new version of the solution. The last block is developed to be able to view the files generated by the solution to re-view the information as a function of time once the data capture is completed, with the aim of sharing and viewing data between teams.

To visualize the solution in full operation, it has been captured in a diagram of modules that generally exemplify the process of visualizing brain signals in real time. In operation you can see 3 important sections, the main one is the module that runs in the Unity game-engine, the second is the real-time brain signal acquisition hardware Emotiv EPOC and the third module refers to the generated products for the solution: i) In

the hardware section you can view the Emotiv EPOC device as it sends brain signals via Bluetooth to the PC, the block that receives, manages, and allows access to said signals is the manufacturer's own (Emotiv Launcher) [13], the Unity module is connected to this block. **ii)** This macro module is made up of two sections, 2d environment and the scripts section. The scripts section exemplifies all the programming carried out, which consists of a Subscription module, which connects to the Emotiv Launcher and manages the data it will obtain, the sending of authentication credentials (since it is a proprietary system, it is necessary to meet the requirements from the manufacturer to access the data) and allows you to read the sections of interest for the application. In this case, the subscribed sections are ECG (encephalogram data), Motion (data on the user's head movement), Facial Expressions (data processed by the launcher that directly allow us to know if the user smiles or grimaces), Mental Commands (they are pre-processed signals training the user to move objects (pull, push, left, right for example) [14]. These signals go directly to the records module which stores the displayed data in volatile memory and then writes the displayed data to files on the hard drive. It should be noted that a marker module has been added, which the user can place as a reference to a stimulus made to the user. tests as a timestamp that identifies this event. The data from the subscription module is also consumed by the serialization values module since it must be transformed into valid formats for later display. The next module through which the serialized data travel is the GameObject UI, which manages the user interface, that is, it allows you to decide the data that will be displayed, change parameters such as the scale in amplitude and function of time, the option has also been placed to numerically visualize the signal together with its 2D visual representation. **iii)** finally, there is the generated product management module which includes the export and import of files in *.CSV and Json format, for later viewing in the application or processing in third-party tools. A database module has also been added so that it can be made available in real time and consumed without the need for file transfers. See Fig. 2.

4 Test

This section describes the methodology used to test the real-time brainwave visualization solution using Emotiv EPOC and Unity. The initial conditions of the experiment, the procedures to follow and how the replicability of the results is guaranteed will be detailed. The testing objective of this solution is the visualization of user

waves in real time without mental, logic or stress testing approach. Only the visualization of its waves will be carried out within the 2D environment and the manipulation of visualization parameters. To continue with the procedure, it is necessary to recalibrate the device with the new test user since everyone is a unique case.

1. Calibration is carried out using the tool provided by the manufacturer (see Fig. 3), Emotiv launcher.

2. It is necessary to place the sensors in the approximate position of the graph until reaching 100% connection (see Fig. 4). It may be necessary to increase the saline levels in each transducer to achieve the green color in all sensors.

3. Now it is necessary to ask the patient to calm down and breathe deeply with his eyes closed, all to achieve 100% signal capture in the ECG (see Fig. 5).

4. Next, run the solution in the Unity environment (see Fig. 6). It is recommended not to create an executable since in the testing stage it may be necessary to make hot adjustments for the correct visualization of the signals.

5. Select the information modules that you want to display in the 2D plane, in this case it will be the ECG and Motion (see Fig. 7).

6. ECG signals can be displayed in 2D line format in time domain, in addition to Motion data in numerical format (see Fig. 8).

7. Press the record button to start capturing the data displayed in the 2D environment.

Finally, the products resulting from the experiment can be viewed for subsequent review and analysis. In the case of replicability, it is detailed that each test is unique, and that the analysis of results focuses on obtaining the final products.

5 Results and Analysis

In this section, the results obtained from real-time brain wave visualization tests using Emotiv EPOC and Unity are presented. The products generated by the solution are described and their implications for future research and applications are analyzed. The successful implementation of the solution has generated the following products:

1. Signal Structure: A complete and structured collection of all brain signals recorded during testing. Includes preprocessed data and relevant metadata in JSON format (see Fig. 9).

2. Excel File for Processing: An Excel file that contains the brain signals ready to process and analyze, contains the values with their respective timestamp, as well as a column in which you can detail the markers made by the investigator (see Fig. 10).

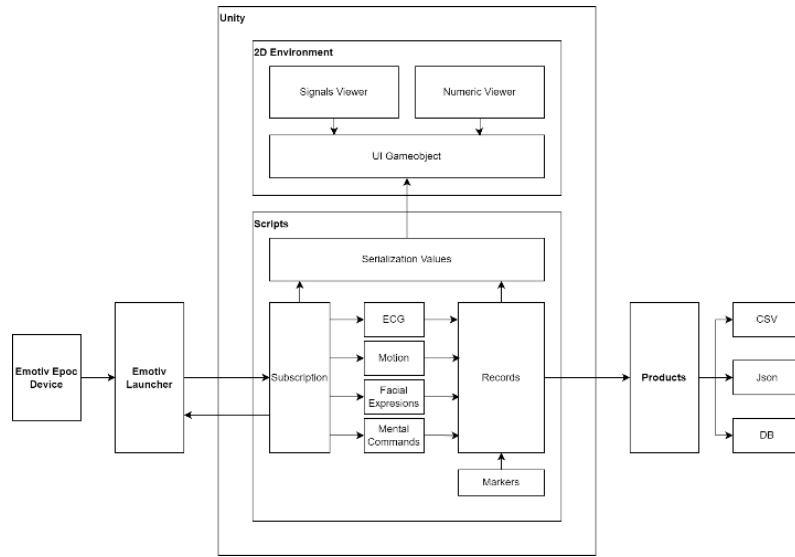


Fig. 2 Main function diagram.

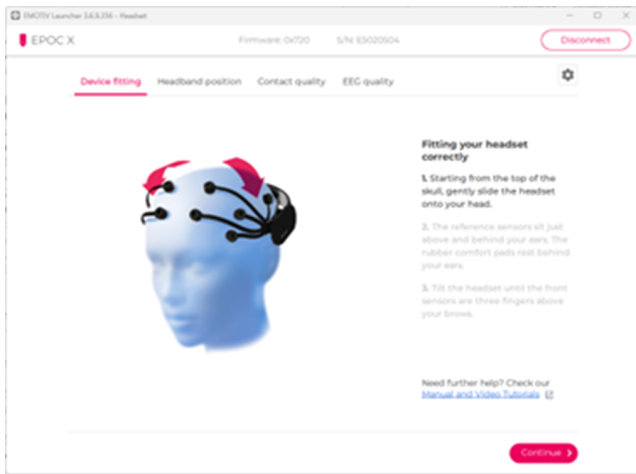


Fig. 3 Configure EMOTIV screen.

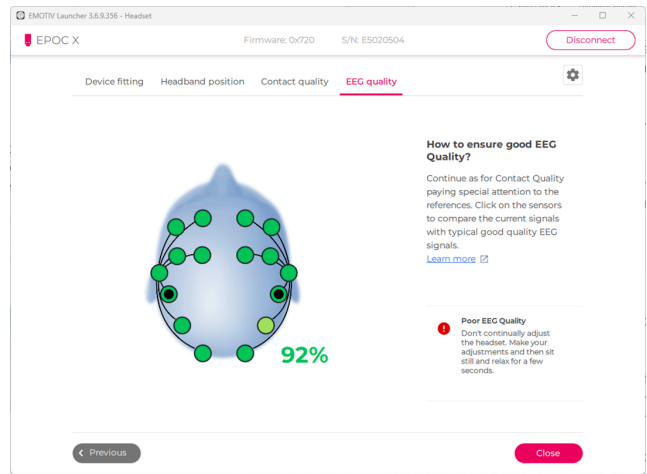


Fig. 5 Check of the ECG Quality status.

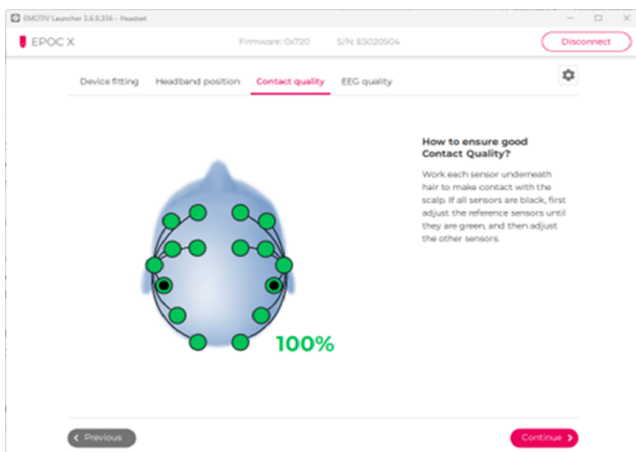


Fig. 4 Dashboard of the 16 sensor status.

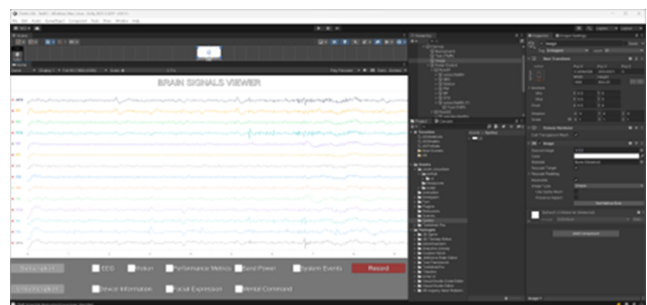


Fig. 6 Unity screen with the proposal.

In addition, you can view one in real time when a file generated by this application is opened. With a time-dependent slider that allows you to recreate the captured signals for greater ease of visualization by the researcher. This animation allows an intuitive under-

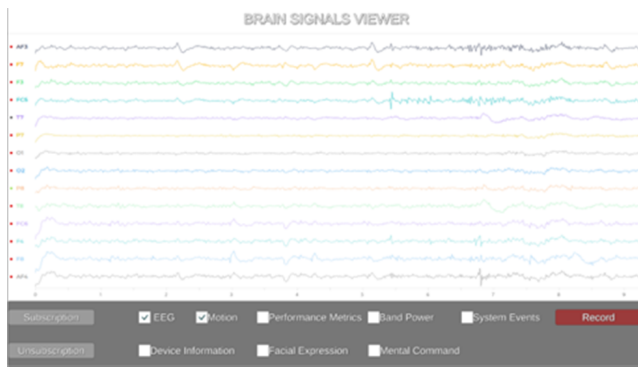


Fig. 7 UI for control the data from EMOTIV.

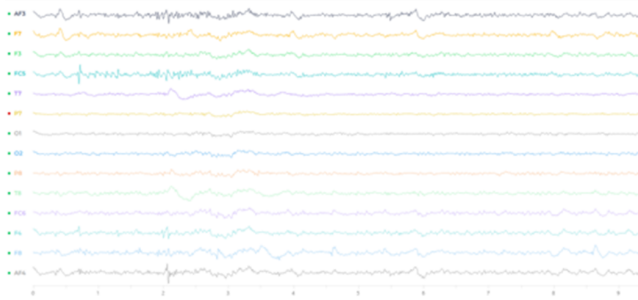


Fig. 8 Graph of signals from EEG in Real-Time.

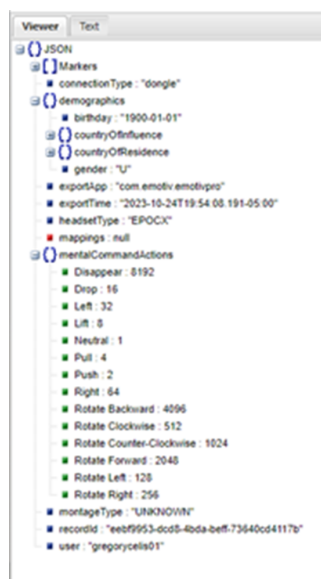


Fig. 9 Data structure in JSON.

standing of the variations in brain activity during the capture of brain signals.

6 Conclusions

Possible directions for future research and applications based on this solution are proposed. The integration of Emotiv EPOC and Unity was successfully achieved

for real-time visualization of brain waves, providing a graphical and interactive representation of brain activity. The generated products, including signal database, ready-to-process Excel file and interactive animation, are useful resources for future research and applications. The solution has significant implications in fields such as brain-computer interface, cognitive therapy and neuroscience research, showing its potential to transform the way we interact with technology and understanding of the human brain.

Conflict of interest

The authors declare that they have no conflict of interest.

References

1. E. I. Olivares, J. Iglesias, C. Saavedra, N. J. Trujillo-Barreto, and M. Valdés-Sosa, "Brain signals of face processing as revealed by event-related potentials," *Behavioural neurology*, vol. 2015, no. 1, p. 514361, 2015.
2. R. A. Ramadan and A. V. Vasilakos, "Brain computer interface: control signals review," *Neurocomputing*, vol. 223, pp. 26–44, 2017.
3. Supriya, Siuly, H. Wang, and Y. Zhang, "An efficient framework for the analysis of big brain signals data," in *Databases Theory and Applications: 29th Australasian Database Conference, ADC 2018, Gold Coast, QLD, Australia, May 24-27, 2018, Proceedings 29*. Springer, 2018, pp. 199–207.
4. M. Strmiska, Z. Koudelková, and M. Žabčiková, "Measuring brain signals using emotiv devices," *WSEAS Transactions on Systems and Control*, 2018.
5. U. Halici, E. Agi, C. Ozgen, and I. Ulusoy, "Analysis and classification of eeg signals for brain computer interfaces," in *International conference on cognitive neuroscience X*, 2008.
6. M. Elgendi, B. Rebsamen, A. Cichocki, F. Vialatte, and J. Dauwels, "Real-time wireless sonification of brain signals," in *Advances in Cognitive Neurodynamics (III) Proceedings of the Third International Conference on Cognitive Neurodynamics-2011*. Springer, 2013, pp. 175–181.
7. W. Srimaharaj, S. Chaising, P. Temdee, R. Chaisricharoen, and P. Sittipraporn, "Brain cognitive performance identification for student learning in classroom," in *2018 Global Wireless Summit (GWS)*. IEEE, 2018, pp. 102–106.
8. R. Y. Karimui, S. Azadi, and P. Keshavarzi, "The adhd effect on the actions obtained from the eeg signals," *Bio-cybernetics and Biomedical Engineering*, vol. 38, no. 2, pp. 425–437, 2018.
9. P. M. Shende and V. S. Jabade, "Literature review of brain computer interface (bci) using electroencephalogram signal," in *2015 International Conference on Pervasive Computing (ICPC)*. IEEE, 2015, pp. 1–5.
10. G. P. Dimitrov, G. S. Panayotova, E. Kovatcheva, D. Borissova, and P. Petrov, "One approach for identification of brain signals for smart devices control." *J. Softw.*, vol. 13, no. 7, pp. 407–413, 2018.

	A	B	C	D	E	F	G	H	I	J	K
1	Timestamp	OriginalTimestamp	EEG.Counter	EEG.Interpolated	EEG.AF3	EEG.F7	EEG.F3	EEG.FC5	EEG.T7	EEG.P7	EEG.O1
2	1.698.012.478.052.480	1.698.012.478.052.960	108.000.000	0.000000	3.785.512.939	3.758.333.252	3.872.564.209	3.841.538.574	4.388.461.426	4.508.205.078	4.524.102.539
3	1.698.012.478.056.380	1.698.012.478.056.770	109.000.000	0.000000	3.787.435.791	3.757.820.557	3.870.897.461	3.843.846.191	4.387.307.617	4.507.948.730	4.525.000.000
4	1.698.012.478.060.290	1.698.012.478.060.570	110.000.000	0.000000	3.793.333.252	3.762.179.443	3.873.461.426	3.850.000.000	4.389.358.887	4.507.948.730	4.526.153.809
5	1.698.012.478.064.190	1.698.012.478.064.570	111.000.000	0.000000	3.801.281.982	3.769.487.061	3.879.743.652	3.857.820.557	4.393.846.191	4.508.077.148	4.526.922.852
6	1.698.012.478.068.100	1.698.012.478.068.580	112.000.000	0.000000	3.809.230.713	3.777.051.270	3.887.692.383	3.864.615.479	4.398.589.844	4.508.077.148	4.526.922.852
7	1.698.012.478.072.000	1.698.012.478.072.480	113.000.000	0.000000	3.815.000.000	3.782.692.383	3.895.000.000	3.868.718.018	4.401.538.574	4.507.948.730	4.526.153.809
8	1.698.012.478.075.910	1.698.012.478.076.390	114.000.000	0.000000	3.817.820.557	3.785.769.287	3.898.974.365	3.869.358.887	4.401.794.922	4.507.563.965	4.525.384.766
9	1.698.012.478.079.810	1.698.012.478.080.290	115.000.000	0.000000	3.817.307.617	3.786.666.748	3.897.692.383	3.867.307.617	4.400.000.000	4.506.794.922	4.524.743.652
10	1.698.012.478.083.710	1.698.012.478.084.200	116.000.000	0.000000	3.814.487.061	3.785.897.461	3.891.281.982	3.864.358.887	4.397.692.383	4.505.512.695	4.523.974.121
11	1.698.012.478.087.620	1.698.012.478.088.000	117.000.000	0.000000	3.811.153.809	3.783.589.844	3.883.589.844	3.862.948.730	4.395.897.461	4.503.974.121	4.522.948.730
12	1.698.012.478.091.520	1.698.012.478.091.900	118.000.000	0.000000	3.809.102.539	3.780.769.287	3.878.846.191	3.863.076.904	4.394.871.582	4.502.820.313	4.522.179.688
13	1.698.012.478.095.430	1.698.012.478.095.810	119.000.000	0.000000	3.809.743.652	3.778.461.426	3.878.974.365	3.862.692.383	4.394.615.234	4.502.436.035	4.522.179.688

Fig. 10 Signals Data in CSV format.

11. K. Holewa and A. Nawrocka, “Emotiv epoc neuroheadset in brain-computer interface,” in *Proceedings of the 2014 15th International Carpathian Control Conference (ICCC)*. IEEE, 2014, pp. 149–152.
12. T. N. Maletе, K. Moruti, T. S. Thapelo, and R. S. Jamisola, “Eeg-based control of a 3d game using 14-channel emotiv epoc+,” in *2019 IEEE International Conference on Cybernetics and Intelligent Systems (CIS) and IEEE Conference on Robotics, Automation and Mechatronics (RAM)*. IEEE, 2019, pp. 463–468.
13. E. Ketola, C. Lloyd, D. Shuhart, J. Schmidt, R. Morenz, A. Khondker, and M. Imtiaz, “Lessons learned from the initial development of a brain controlled assistive device,” in *2022 IEEE 12th Annual Computing and Communication Workshop and Conference (CCWC)*. IEEE, 2022, pp. 0580–0585.
14. E. Crespi, D. E. Cerioli, A. Gentili, F. Carloni, and M. D. Santambrogio, “Braintrack: A replicable and accessible methodology for customized brain-machine interface applications,” in *2022 IEEE 7th Forum on Research and Technologies for Society and Industry Innovation (RTSI)*. IEEE, 2022, pp. 129–135.

License

Copyright (2024) © Celis Gregory, Washington X. Quevedo.

This text is protected under an international Creative Commons 4.0 license.



You are free to share, copy, and redistribute the material in any medium or format — and adapt the document — remix, transform, and build upon the material — for any purpose, even commercially, provided you comply with the conditions of Attribution. You must give appropriate credit to the original work, provide a link to the license, and indicate if changes were made. You may do so in any reasonable manner, but not in a way that suggests endorsement by the licensor or approval of your use of the work.

License summary - Full text of the license

Early Fault Detection in Paper Machine Motors Using Machine Learning

Cristian P. Chuchico · Oscar Acosta Agudelo

Received: 18 Feb 2024 / Accepted: 02 May 2024 / Published: 16 May 2024

Abstract: This research addresses the application of a neural network as a tool for early fault detection in the motors of a paper machine under a simulated environment. It proposes the analysis of variables from a torque control loop. The data for training and validating the model is obtained through the simulation of Direct Torque Control (DTC) of an AC motor in Simscape within Simulink. Both normal and faulty operating modes are considered. Under these two scenarios, various speed setpoints are configured, and the necessary data for training the developed model is collected.

Keywords Machine Learning · Predictive Maintenance · Paper Machine · DTC · Simscape


1 Introduction

In the industrial sector, especially in areas like paper manufacturing where operational efficiency and process continuity are paramount, equipment maintenance plays a crucial role in the success and profitability of operations. Maintenance management is sometimes conducted traditionally with manual records and data entry in spreadsheets, methodologies that have yielded good results for industrial production [1]. However, this approach involves several issues, such as human errors in data collection and record entry, the frequency of maintenance plan execution, among others. Therefore, the ability to effectively prevent unexpected motor failures remains a significant challenge [2][3].

Moreover, artificial intelligence has seen broad evolution across diverse fields, including service sectors, healthcare [4], robotics [5], and the industrial domain. In this context, predictive maintenance, supported by advances in technologies such as machine learning, could emerge as a strategy to ensure the availability and reliability of industrial assets and processes [6][7]. For instance, [8] shows the application of neural network classifiers is proposed for detecting anomalies such as specks and various types of diffraction in a laser beam. The research achieves an accuracy of around 99% with very short processing times, aiming to reduce reliance on an expert for beam evaluation. Moreover, a review of ML technologies related to predictive maintenance of conveyor belts is conducted in [9], summarizing the results and challenges of various methodologies used in these systems. In addition, [10] shows a multihead neural network developed under the variability of individual machine degradations to derive machine-level prognostics. This network learns degradation features and updates remaining useful lifetime (RUL) distributions from diverse distribution ensembles. Even though these articles are closely related to the paper manufacturing sector, a comprehensive analysis using artificial intelligence to extend the useful life of engines might still be unresolved.

In this work, a machine learning algorithm is incorporated into the predictive maintenance of the drive motors of a paper machine. The aim is to provide a tool that facilitates the early diagnosis of anomalies in motor operation, thereby preventing mechanical damage to couplings, crosses, and cardan shafts in the system. With the incorporation of this tool, the information from operating variables such as speed reference, speed feedback, motor current, torque reference, and motor torque (calculated based on motor voltage and current) is analyzed. This analysis helps determine whether the machine's operation is adequate or if there is a need to plan activities to address out-of-standard conditions, thereby avoiding unplanned production stoppages [11][12]. The document presents the result of a direct torque

Cristian P. Chuchico 
Escuela de Ingeniería y Tecnología
International University of La Rioja
La Rioja, Spain
Tel.: +593 992842517
E-mail: cristianpaul.chuchico050@comunidadunir.net

Oscar Acosta Agudelo 
Escuela de Ingeniería y Tecnología
International University of La Rioja
La Rioja, Spain
E-mail: oscarsneider.acosta-externo@unir.net

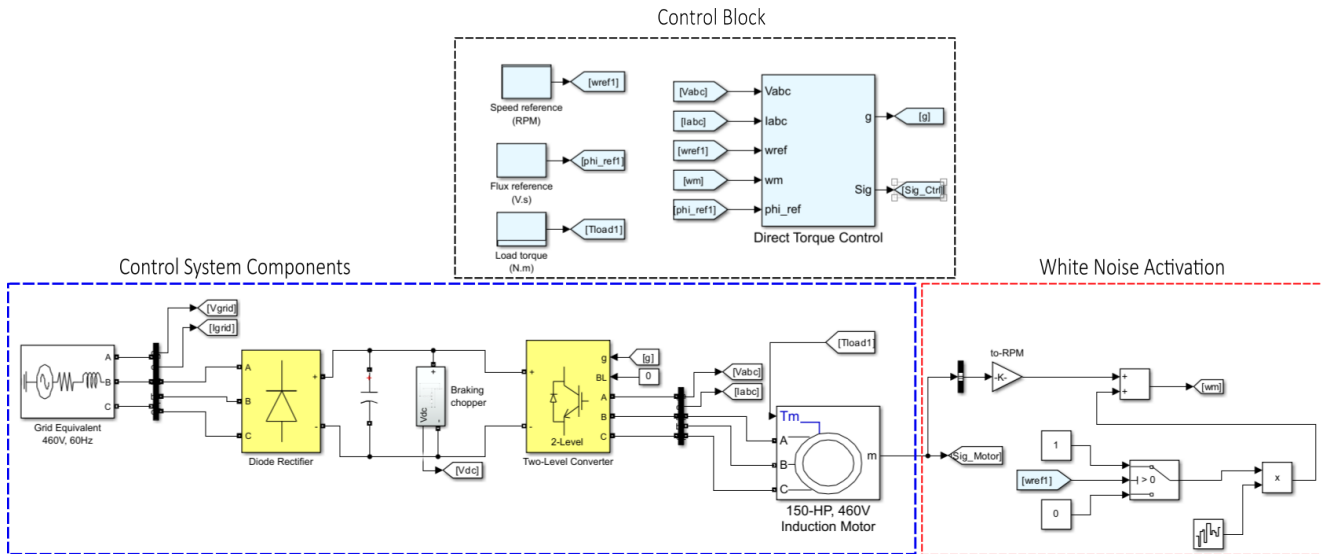


Fig. 1 Direct Torque Control (DTC) system.

control (DTC) simulation of a three-phase motor using Simscape in MATLAB [13], from which the parameters for training the neural network are obtained [14]. The main contribution of this work is the incorporation of a neural network for anomaly detection in motors in the paper industry. By validating the contribution of this neural network, it is possible to integrate the algorithm into a real production environment and connect it to the SCADA system via an OPC server, simplifying signal interpretation and contributing to industrial maintenance management.

2 Neural Network Configuration and Training

2.1 Simulation Scenario Setup

For the implementation of the simulation environment, Simscape Electrical blocks are used, starting with one of the direct torque control (DTC) exercises available on the official MathWorks website [15]. The main blocks within the simulated environment are: the direct torque controller, the noise signal activation, and the elements that emulate the physical system: power supply, rectifier block, inverter, and motor. Fig. 1 shows the cited setup and its connections.

2.2 Data Generation for Training

As described in Table 1, during the model simulations, different combinations of speed and torque are applied by using step signals at specific time intervals at the controller inputs, see Figure 2.

Once the controller's operation has been verified, a simulation is run with the same speed and torque setpoints, incorporating random noise in the system feedback to emulate abnormal system behavior. The results shown in Figure 3 indicate that the controller exhibits highly oscillatory behavior.

The simulation behavior aligns with mechanical issues encountered in a real system, as shown in Figure 4. The figure displays the torque of four motors: motors a and b are operating normally, while motors c and d exhibit signals from systems with mechanical problems.

The data for the analysis are obtained from several simulations, which include different scenarios such as acceleration, deceleration, and steady state. The training of the algorithm is based on identifying the behavior of the torque control loop variables. For this purpose, 6 variables are considered, from which a total of 533310 samples are obtained. The analyzed variables are:

- Set Point or speed reference in RPM.
- Motor speed feedback.
- Set point or torque reference.
- Torque control signal (controller output).
- Motor torque.
- Motor current.

2.3 Neural Network Training

The process is divided into several trials to define the best parameters for the neural network, with the configurations shown in Table 2. After the training process, the model's performance is evaluated using confusion matrices for each trial, allowing us to visualize the model's ability to correctly classify normal and

Table 1 Example of applied speed and torque combinations.

step	Operation State	Torque Ref	Torque Motor	Speed Ref
T1	Null	Null	Null	Null
T2	Acceleration	Null	Over Reference	0 to 1200 RPM
T3	Stable	600 and 100 Nm	According with reference	1200 RPM
T4	Deceleration	100 Nm	Under reference	1200 to 500 RPM
T5	Stable	100 Nm	According with reference	500 RPM
T6	Acceleration & Stable	100 Nm	Over and according with reference	500 to 700 RPM

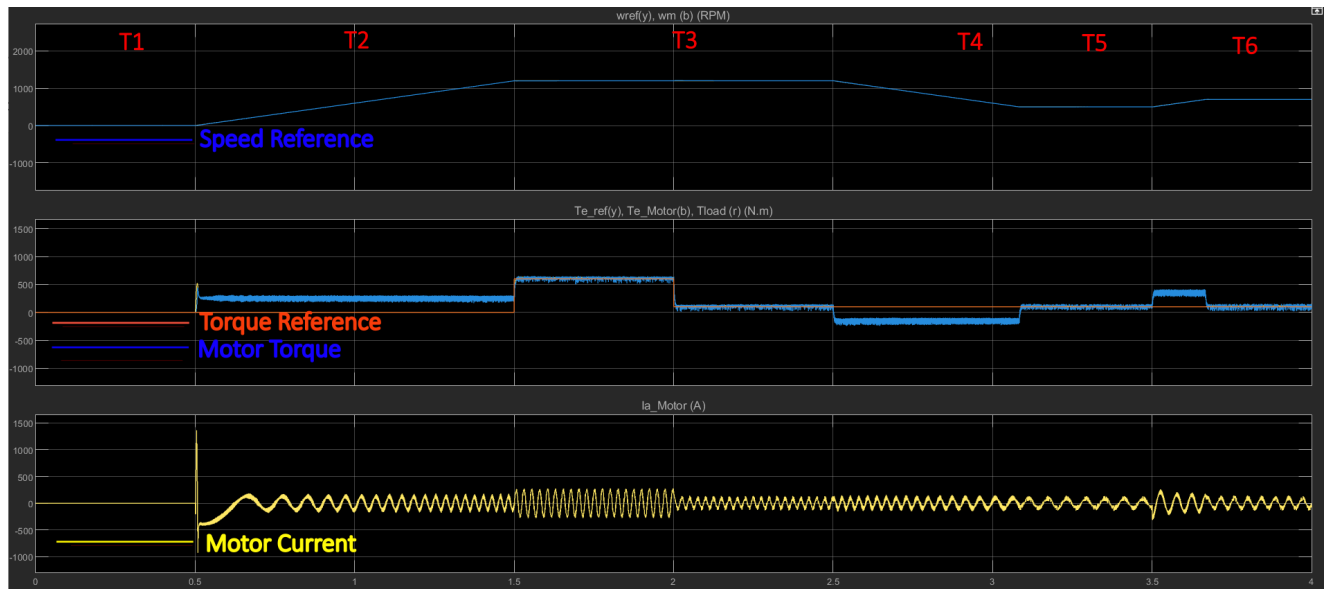


Fig. 2 Direct Torque Control loop response, normal operating conditions.

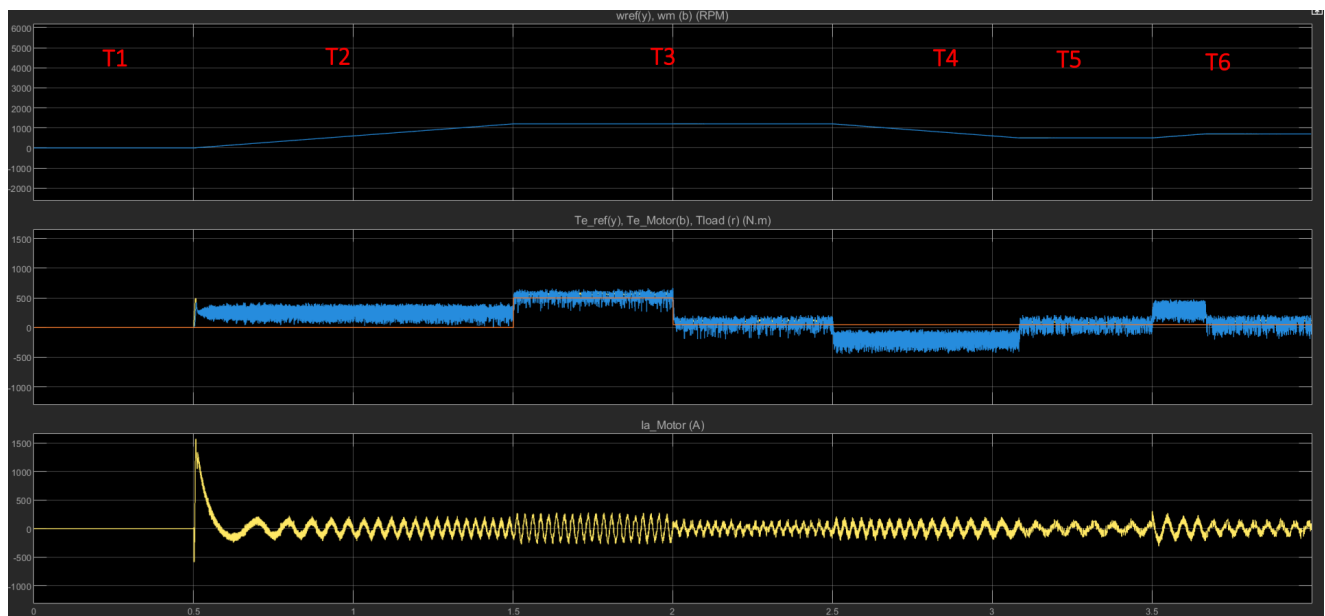


Fig. 3 Direct Torque Control loop response, operating conditions with noise.

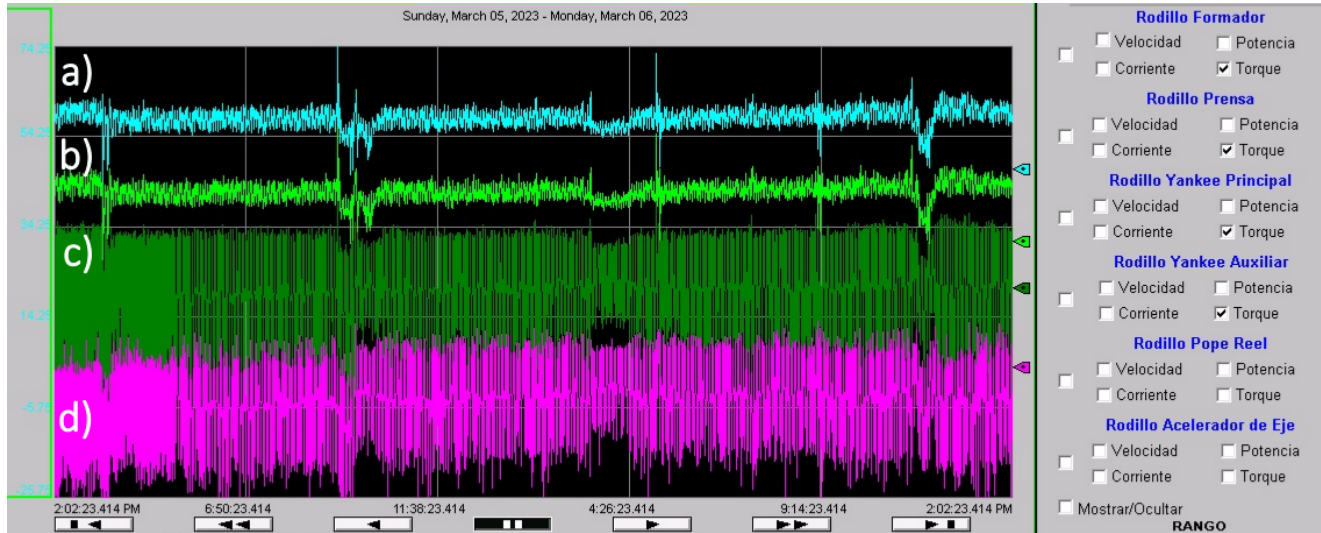


Fig. 4 Torque trends of 4 motors: a) and b) normal operation, c) and d) with mechanical issues.

faulty operating states of the system. The results of each trial conducted are presented below: In the first trial, the confusion matrix (Figure 5) shows that the model achieved a 70.3% accuracy. In the second trial, whose results are presented in the confusion matrix in Figure 6, the model's consistency was confirmed, and a 72.7% accuracy was achieved. Subsequently, in Trial 3, an increase in the input data was made, and three previous samples were considered for analysis. That is, to determine the system's performance at time t_0 , the values corresponding to t_{-3} , t_{-2} , t_{-1} , and t_0 were taken into account. Therefore, if the same variables are considered for each moment in time, the number of neurons in the input layer will be 24. With the changes considered, a 73.9% accuracy was achieved, and the model's ability to distinguish between normal and faulty states improved (Figure 7). In Trial 4, the algorithm's robustness and its ability to generalize from the training data were demonstrated, achieving the best performance (Figure 8). For Trial 5, an adjustment was made to the data allocation as follows: 70% for training and 30% for testing, in order to evaluate whether the algorithm maintains its performance and to rule out overfitting of the network (Figure 9).

3 Metrics Calculation

Based on the developed trials, precision, accuracy, and recall are calculated, considering the values of true positives (TP), false positives (FP), false negatives (FN), and true negatives (TN) shown in each of the confusion matrices from the previous section. Accuracy indicates the proportion of correct predictions and is defined as (1):

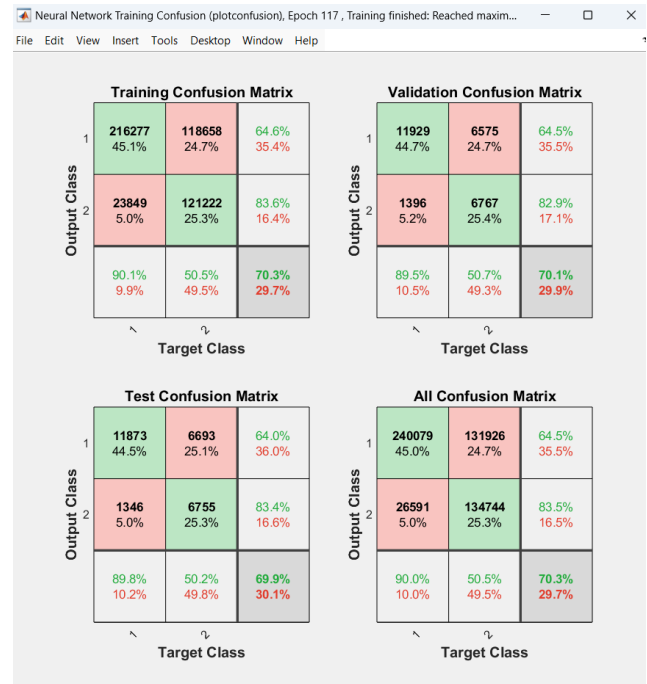


Fig. 5 Confusion matrix, Trial 1

$$accuracy = \frac{TP + TN}{TP + TN + FP + FN} \quad (1)$$

Precision shows the proportion of correct positive predictions. (2):

$$precision = \frac{TP}{TP + FP} \quad (2)$$

Recall indicates the proportion of actual positives that have been correctly predicted. (3):

Table 2 Configuration of the conducted trials.

Trial	Input layer size	Hidden layer size	Output layer size	Training-validation sample split
Trial 1	6	2	2	90 - 10
Trial 2	6	5	2	90 - 10
Trial 3	24	1	2	90 - 10
Trial 4	24	3	2	90 - 10
Trial 5	24	3	2	70 - 30

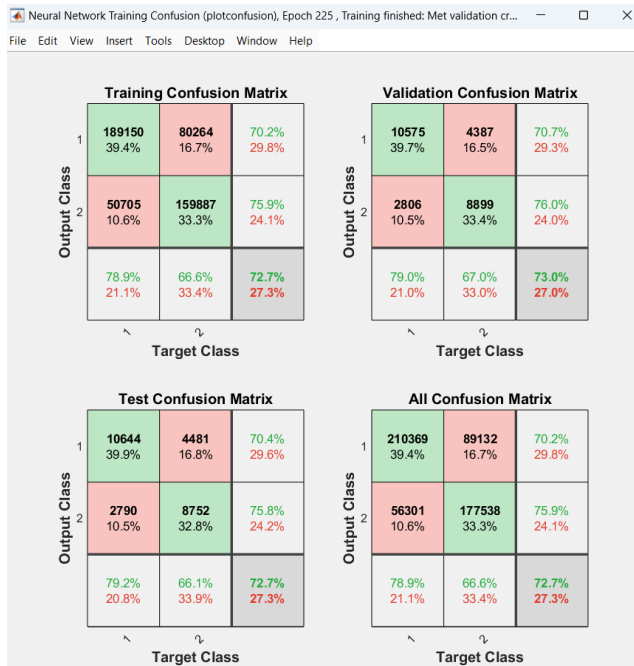


Fig. 6 Confusion matrix, Trial 2.



Fig. 8 Confusion matrix, Trial 4.



Fig. 7 Confusion matrix, Trial 3.



Fig. 9 Confusion matrix, Trial 5.

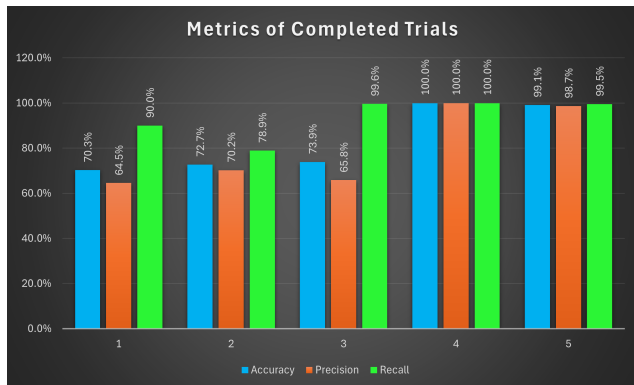


Fig. 10 Metrics calculated for each trial conducted.

$$recall = \frac{TP}{TP + FN} \quad (3)$$

Using the values obtained in (see Sect. 2.3) and according to (1), (2), and (3), the metrics for each of the trials are obtained (Fig. 10). The best performance of the neural network is achieved with the structure proposed in Trial 4. Finally, in Trial 5, this structure is maintained, but the percentage of samples assigned for training is set to 70% and for validation to 30%. Under these conditions, precision reaches 98.7%, accuracy 99.1%, and recall 99.5%, indicating that the algorithm performs well under the proposed scenario and conditions

4 Conclusions

The main contribution of this work is the application of a neural network for the early detection of faults based on the analysis of variables from a direct torque control (DTC) system. Using Simscape in MATLAB, the simulation environment was configured, and the necessary data for model training was generated. It has been demonstrated that the developed system can satisfactorily identify normal and fault conditions with an accuracy exceeding 99%, confirming the effectiveness of the adopted approach and highlighting the potential of machine learning to enhance predictive maintenance in industrial environments.

As shown in the development of this proposal, it is possible to design a machine learning algorithm that continuously analyzes motor operation variables without interfering with daily production activities, providing a basis for future research and practical applications related to optimizing control systems and reducing operational costs through early fault detection.

Conflict of interest

The authors declare that they have no conflict of interest.

References

1. G. M. M. Fernandez Cabanas Manés, *Técnicas para el mantenimiento y diagnóstico de máquinas eléctricas rotativas*. Gran via de les Corts Catalanes, 594 08007 Barcelona: Marcombo, 1998.
2. J. L. Zhe Li, Qian He, “A survey of deep learning-driven architecture for predictive maintenance,” *Engineering Applications of Artificial Intelligence*, vol. 133, 2024.
3. M. J. Gupta Suraj, Kumar Akhilesh, “A critical review on system architecture, techniques, trends and challenges in intelligent predictive maintenance,” *Safety Science*, vol. 177, 2024.
4. J. Buele, F. A. Chicaiza, M. León, and A. P. Sánchez, “Virtual rehabilitation system for fine motor skills using artificial neural networks,” in *IOP Conference Series: Materials Science and Engineering*, vol. 1070, no. 1. IOP Publishing, 2021, p. 012054.
5. E. Slawiński, F. Rossomando, F. A. Chicaiza, J. Moreno-Valenzuela, and V. Mut, “Lstm network in bilateral teleoperation of a skid-steering robot,” *Neurocomputing*, p. 128248, 2024.
6. R. Dagner, “Machine learning para mejorar la gestión de mantenimiento de máquinas industriales,” *Universidad Cesar Vallejo*, 2021.
7. Y. U. Muhammed Fatih Pekşen, Ulaş Yurtsever, “Enhancing electrical panel anomaly detection for predictive maintenance with machine learning and iot,” *Alexandria Engineering Journal*, vol. 96, pp. 112–123, 2024.
8. G. P. Mostowski Daniel, Jakubczak Krzysztof, “Automated laser beam characterization using artificial intelligence (ai) for the predictive maintenance of lasers,” *Optics and Laser Technology*, 2024.
9. k. R. Santoshi Anusha, “Digital transformation technologies for conveyor belts predictive maintenance: a review,” *Indonesian Journal of Electrical Engineering and Computer Science*, pp. 639–646, 2024.
10. Y. D. Tangbin Xia, Yimin Jiang, “Intelligent maintenance framework for reconfigurable manufacturing with deep-learning-based prognostics,” *IEEE Internet of Things Journal*, vol. 11, 2024.
11. B. Patrik, “Smart condition monitoring using machine learning,” *SPE Middle East Intelligent Oil and Gas Symposium*, 2017.
12. L. R. J. R. C. R. A. Guerrero Cano Manuel, Luque Sendra Amalia, “Predictive maintenance using machine learning techniques,” *Alexandria Engineering Journal*, vol. 96, pp. 112–123, 2024.
13. Mathworks®, “Simscape,” la.mathworks.com/products/simscape.html, 2024, accedido en junio de 2024.
14. L. S. J. Alfonso, “Deep learning: teoría y aplicaciones,” *Alpha Editorial*, vol. 1, pp. 93–95, 2021.
15. Mathworks®, “Direct torque control of an induction motor drive,” <https://la.mathworks.com/help/sps/ug/power-motordrive-IM-DTC-HYST.html>, 2024, accedido en junio de 2024.

License

Copyright (2024) © Cristian P. Chuchico, Oscar Acosta Agudelo.

This text is protected under an international Creative Commons 4.0 license.



You are free to share, copy, and redistribute the material in any medium or format — and adapt the document — remix, transform, and build upon the material — for any purpose, even commercially, provided you comply with the conditions of Attribution. You must give appropriate credit to the original work, provide a link to the license, and indicate if changes were made. You may do so in any reasonable manner, but not in a way that suggests endorsement by the licensor or approval of your use of the work.

[License summary](#) - [Full text of the license](#)